frontiers in Marine Science

ORIGINAL RESEARCH
published: 17 March 2021
doi: 10.3389/fmars.2021.638505

# A Microbial Nitrogen Engine Modulated by Bacteriosyncytia in Hexactinellid Sponges: Ecological Implications for Deep-Sea Communities

*Manuel Maldonado*[1]*, *María López-Acosta*[1], *Kathrin Busch*[2], *Beate M. Slaby*[2], *Kristina Bayer*[2], *Lindsay Beazley*[3], *Ute Hentschel*[2,4], *Ellen Kenchington*[3] and *Hans Tore Rapp*[5†]

[1] Department of Marine Ecology, Center for Advanced Studies of Blanes (CEAB-CSIC), Girona, Spain, [2] GEOMAR Helmholtz Centre for Ocean Research Kiel, Kiel, Germany, [3] Department of Fisheries and Oceans, Bedford Institute of Oceanography, Dartmouth, NS, Canada, [4] Unit of Marine Symbioses, Christian-Albrechts University of Kiel, Kiel, Germany, [5] Department of Biological Sciences, University of Bergen, Bergen, Norway

OPEN ACCESS

**Edited by:**
Lorenzo Angeletti,
Institute of Marine Science (CNR), Italy

**Reviewed by:**
Robert W. Thacker,
Stony Brook University, United States
Cole G. Easson,
Middle Tennessee State University, United States
Fengli Zhang,
Shanghai Jiao Tong University, China
Giorgio Bavestrello,
University of Genoa, Italy

***Correspondence:**
Manuel Maldonado
maldonado@ceab.csic.es

†Deceased

**Specialty section:**
This article was submitted to Deep-Sea Environments and Ecology, a section of the journal Frontiers in Marine Science

**Received:** 06 December 2020
**Accepted:** 16 February 2021
**Published:** 17 March 2021

**Citation:**
Maldonado M, López-Acosta M, Busch K, Slaby BM, Bayer K, Beazley L, Hentschel U, Kenchington E and Rapp HT (2021) A Microbial Nitrogen Engine Modulated by Bacteriosyncytia in Hexactinellid Sponges: Ecological Implications for Deep-Sea Communities. Front. Mar. Sci. 8:638505. doi: 10.3389/fmars.2021.638505

Hexactinellid sponges are common in the deep sea, but their functional integration into those ecosystems remains poorly understood. The phylogenetically related species *Schaudinnia rosea* and *Vazella pourtalesii* were herein incubated for nitrogen and phosphorous, returning markedly different nutrient fluxes. Transmission electron microscopy (TEM) revealed *S. rosea* to host a low abundance of extracellular microbes, while *Vazella pourtalesii* showed higher microbial abundance and hosted most microbes within bacteriosyncytia, a novel feature for Hexactinellida. Amplicon sequences of the microbiome corroborated large between-species differences, also between the sponges and the seawater of their habitats. Metagenome-assembled genome of the *V. pourtalesii* microbiota revealed genes coding for enzymes operating in nitrification, denitrification, dissimilatory nitrate reduction to ammonium, nitrogen fixation, and ammonia/ammonium assimilation. In the nitrification and denitrification pathways some enzymes were missing, but alternative bridging routes allow the microbiota to close a N cycle in the holobiont. Interconnections between aerobic and anaerobic pathways may facilitate the sponges to withstand the low-oxygen conditions of deep-sea habitats. Importantly, various N pathways coupled to generate ammonium, which, through assimilation, fosters the growth of the sponge microbiota. TEM showed that the farmed microbiota is digested by the sponge cells, becoming an internal food source. This microbial farming demands more ammonium that can be provided internally by the host sponges and some 2.6 million kg of ammonium from the seawater become annually consumed by the aggregations of *V. pourtalesii*. Such ammonium removal is likely impairing the development of the free-living bacterioplankton and the survival chances of other sponge species that feed on bacterioplankton. Such nutritional competitive exclusion would favor the monospecific character of the *V. pourtalesii* aggregations. These aggregations also affect the surrounding environment through an annual release of 27.3 million kg of nitrite and, in smaller quantities, of nitrate and phosphate. The complex metabolic integration

among the microbiota and the sponge suggests that the holobiont depends critically on the correct functioning of its N-driven microbial engine. The metabolic intertwining is so delicate that it changed after moving the sponges out of their habitat for a few days, a serious warning on the conservation needs of these sponge aggregations.

**Keywords: sponge physiology, sponge microbiota, nitrogen cycling, phosphorous cycling, functional deep-sea ecology, benthic-pelagic coupling, sponge aggregations, nutritional competitive exclusion**

## INTRODUCTION

Glass sponges (phylum Porifera, class Hexactinellida) are marine organisms markedly restricted to the deep sea (Tabachnick, 1994), with only a handful of species that can be found at SCUBA-diving depths (Mackie and Singla, 1983; Vacelet et al., 1994; Cook et al., 2008). Such bathymetric confinement has hindered empirical investigations on this large sponge lineage, the physiology and functional ecology of which remains poorly understood. During the last two decades, the advent of high-capacity remote operated vehicles (ROVs) has opened deep-sea communities to experimental and manipulative research, making it possible to approach the physiology of the organisms and their functional integration into the deep-water ecosystems.

At bathyal depths, hexactinellid sponges can occur forming dense and extensive aggregations (reviewed in Maldonado et al., 2017). While the physical presence of the sponges increases the 3D-complexity of the habitats (Beazley et al., 2013; Dunham et al., 2018; Hawkes et al., 2019), their physiological activity also carries an exchange of organic and inorganic nutrients with the surrounding environment (Pile and Young, 2006; Yahel et al., 2007; Kahn et al., 2018). Such nutrient exchange is foreseen to affect the surrounding deep-sea system in a multiplicity of ways, but the exact mechanisms behind it, as well as the magnitude of the net fluxes, remain poorly investigated, at least in comparison with the information available for shallow-water demosponges (reviewed in Maldonado et al., 2012 and Zhang et al., 2019). The implications of the hexactinellid aggregations on the cycling of silicon have been demonstrated at regional oceanographic levels (Chu et al., 2011; Maldonado et al., 2021), but their role in respect to the flux of nitrogen (N) and phosphorous (P) nutrients remains less understood. Traditionally, hexactinellid sponges have been interpreted as long-lived organisms with low rates of physiological activity, so that the net flux rates of nutrient exchange with the environment were *a priori* expected to be modest. However, while the rates of silicon utilization depend directly on the metabolic activity of the sponge cells, the net flux of N and P inorganic nutrients of the sponges depend on the metabolic activity not only of the sponge cells but also of the microbial populations (the microbiota) that the sponges host. From studies on shallow-water demosponges, it is well-known that the "holobiont" constituted by a sponge and its microbiota is able to either incorporate or release a variety of dissolved inorganic nutrients such as ammonium, nitrate, nitrite, and phosphate, depending on the sponge species (Diaz and Ward, 1997; Maldonado et al., 2012; Ribes et al., 2012; Fiore et al., 2013; Keesing et al., 2013; Hoer et al., 2018; Pita et al., 2018; López-Acosta et al., 2019; Zhang et al., 2019). Often the microbial communities hosted by demosponges are complex and may include simultaneously archaea and bacteria, including cyanobacteria. Demosponges with high abundance of microbes in their tissues (i.e., HMA sponges) often —but not always (Bayer et al., 2008)— take up ammonium from seawater, which is a N source for chemo- and phototrophic bacteria and an energy source for ammonia-oxidizing bacteria (AOB) and archaea (AOA). In contrast, the HMA demosponges typically release nitrate and nitrite, as the probable result of the metabolic activity of nitrifying symbiotic bacteria (Corredor et al., 1988). The demosponges with low abundance of associated microbes (LMA sponges) are typically net sources of both nitrate and nitrite as well, and, in many cases, also release ammonium (Jiménez and Ribes, 2007; Southwell et al., 2008a,b; Morganti et al., 2017). Most investigated demosponges —but not all— are net sources of phosphate, which is released at very low rates (Maldonado et al., 2012; Ribes et al., 2012; López-Acosta et al., 2019).

In this regard, there is no comprehensive information for hexactinellids about the sign and magnitude of the net flux of ammonium, nitrite, nitrate and phosphate. Given the idiosyncrasy of the syncytial tissues of hexactinellids, it is not even clear whether these sponges can be objectively identified as belonging to either the HMA or LMA models established for demosponges and, if so, it remains to be described where the abundance of microbes would be located within their body, typically consisting of large internal aquiferous spaces and only very thin threads of tissue (i.e., epithelia + mesohyl) attached to the siliceous skeleton. A recent study of South Pacific deep-sea sponges, including demosponges and hexactinellids, has reported microbial communities in hexactinellids that appear to show patterns equivalent to the LMA-HMA dichotomy known for shallow-water demosponges (Steinert et al., 2020). Likewise, a recent pioneering study (Tian et al., 2016) on the hexactinellid *Lophophysema eversa* has reported the microbial community to be dominated by chemoautotrophic bacteria, mostly ammonia-oxidizing archaea (AOA), nitrite-oxidizing bacteria (NOB), and sulfur-oxidizing bacteria (SOB). These three functional groups of microbes were interpreted as playing roles in the cycling of carbon, nitrogen and sulfur in the micro-environment inside the sponge body, being scavengers of toxic ammonia, nitrite and sulfide waste produced by the metabolism of the sponge cells in the conditions of the deep-sea environment. The NOB groups also appear to participate in pathways that lead to production of vitamin B12 (Tian et al., 2016). In a recent study on the hexactinellid *Vazella pourtalesii*, the microbiome has been well-characterized through genomic approach, as well as the functional traits that allow the microbes to survive and

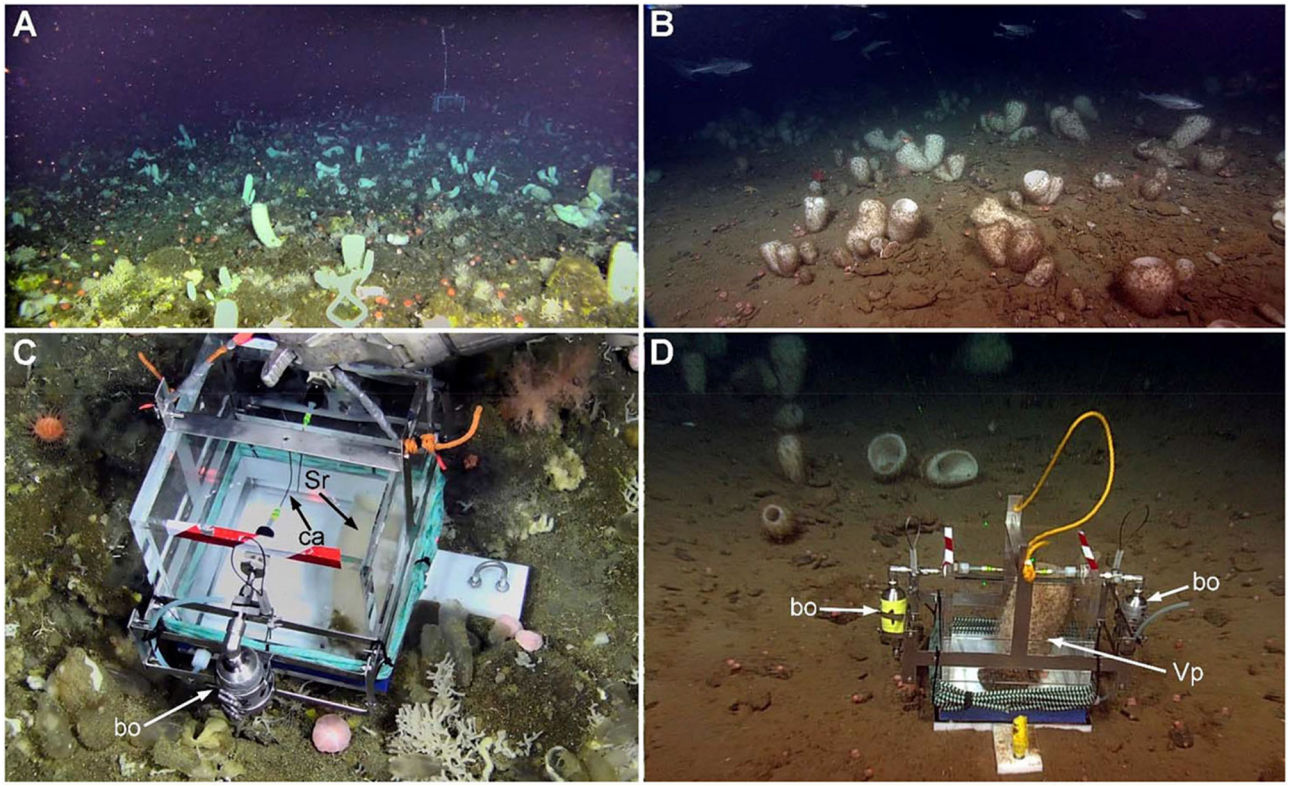


**FIGURE 1 | (A)** View of a multi-species sponge community at the Schulz Bank seamount (located between the Greenland and Norwegian Seas; 73.8 °N; 7.5 °E), where the whitish tubes of the hexactinellid *Schaudinnia rosea* co-dominate in abundance along with a variety of demosponges and small cnidarians. **(B)** View of the monospecific aggregations of the hexactinellid *Vazella pourtalesii* that extend on the deep region of the continental shelf in Nova Scotia (Canada). **(C,D)** *In-situ* incubation of an individual of *Schaudinnia rosea* (Sr) and a *Vazella pourtalesii* (Vp) in their respective natural communities at depths of 580 and 180 m, respectively. Note that the incubation chambers incorporate two external steel bottles (bo) for water sampling within the camera by means of capillaries (cp) that pierce the chamber wall.

proliferate within the sponge tissue (Bayer et al., 2020). In the current study, we attempt to integrate the genomic microbial information in a physiological and ecological context to better understand the nitrogen and phosphorus fluxes of the sponges, what sponge capabilities may rely on the metabolic integration with their microbes, and what the implications are for the deep-sea ecosystem where aggregations of these hexactinellid sponges occur.

To this aim, in the frame of the EU H2020 project "SponGES," we have investigated two ecologically important deep-sea hexactinellid sponge species, *Schaudinnia rosea* (Fristedt, 1887) and *Vazella pourtalesii* (Schmidt, 1870). In both cases, the sponges form dense aggregations, representing relevant community components at both the physical and the functional levels. We have quantified *in situ* the net flux rates of ammonium, nitrate, nitrite, and phosphate, using benthic incubation chambers manipulated by high-capacity ROVs. By collecting live animals, net flux rates were also measured in laboratory experiments for one of the species, namely *V. pourtalesii*. Through metagenomic analysis, the main microbial lineages occurring within the sponges have been revealed along with their functional implication in a variety of relevant biochemical routes in the N and P metabolism. Through ultrastructural research, the particular locations of the microbes within the sponge body have also been unveiled. Therefore, this study seeks to contribute to a better understanding of (1) the mechanisms behind the nutrient flux rates of hexactinellid sponges and (2) the ecological significance of those fluxes to the deep-sea ecosystems.

## MATERIALS AND METHODS

### Sponge Species

The studied hexactinellid sponges, *S. rosea* and *V. pourtalesii*, are phylogenetically closely related, both belonging to the subfamily Rossellinae in the family Rossellidae. The species *S. rosea* is distributed along the Arctic Ocean from 90 to 3110 m depth. This species becomes co-dominant in abundance at the Schulz Bank, a seamount located on the Arctic Mid-Ocean Ridge (73.8 °N; 7.5 °E) between the Greenland and Norwegian Seas. There it forms, along with several demosponges, a sponge-dominated benthic community that extends over the top of the seamount at depths of 550–600 m (**Figure 1A**, **Supplementary Video 1**). The species *V. pourtalesii* occurs in the northwest Atlantic, from 100 to 935 m depth. This species is mostly known from dense, monospecific aggregations (**Figure 1B**, **Supplementary Video 2**) extending on the deep continental shelf of Nova Scotia (Canada) at 150–200 m deep (Beazley et al., 2018; Maldonado et al., 2021). At those depths, the areas of the Scotian continental

shelf where the sponge aggregations occur are an aphotic environment with bottom water temperatures below the 10°C permanent thermocline, features favored by the high latitude. Those conditions, according to a functional definition of the deep-sea (Gage and Tyler, 1991), qualify the *Vazella* grounds as a deep-sea habitat despite being topographically located on the continental shelf.

## Field Incubations of Sponges

We built 6 benthic incubation chambers in methyl methacrylate and inox steel, with an incubation volume of either 17.3 or 13.3 L (as described in Maldonado et al., 2020). Chambers incorporated a floor piece of Delrin acetal resin, which allowed for the incubation of sponges in isolation from the external environment. This approach avoided interference by nutrient fluxes from the resuspended sediments that occurred during deployments and ROV activity on the sea bottom. The chambers incorporated two external sampling bottles (120 mL) made of steel and internally folded with polytetrafluoroethylene (**Figures 1C,D**). Through a steel capillary (20 cm long and 0.6 mm wide) that pierced the wall of the chamber, each bottle was designed to collect a water sample (under negative pressure conditions) from inside the incubation chamber while it was opened for 5 min and then closed using the ROV manipulator arms (**Figures 1C,D**).

*In-situ* incubations were conducted during two oceanographic cruises. In August 2018, on board of R/V GO Sars and using the ROV ÆGIR 6000, we incubated seven individuals of *S. rosea* (**Supplementary Video 3**) and a control on the Schultz Massif seamount, at depths of 577–580 m. In September 2017, on board of CCGS Martha L Black and using the ROV ROPOS, a total of four individuals of *V. pourtalesii* and a control (see below) were incubated *in situ* on the Scotian Shelf at depths of 160–180 m (**Supplementary Video 4**), as described in Maldonado et al. (2020). The number of incubations was limited by inclement weather in the area during the entire cruise. For the incubations, each sponge was grabbed by the manipulator arm from the small rock on which it was attached, then placed on the floor piece of the incubation chamber, and covered with the methyl methacrylate box, which rested into a groove in the floor piece designed to prevent leakages from the incubation unit. Once the sponge was inside the chamber and the chamber properly sealed, one of the sampling bottles was opened to collect water for 5 min and then closed again to avoid water exchange with the surrounding seawater. As a control, we used a rock selected from the sponge grounds but without an attached sponge. After an incubation period of 19–28 h (incubation time varied due to weather and the logistics of the cruises), the ROV returned to the chamber position and triggered the second sampling bottle. After this second water collection, the sponge and its attachment rock were collected to estimate volume and biomass, needed to normalize N and P flux rates by sponge volume (mL); sponges were later combusted for flux rates to be also normalized by ash-free dry weight (AFDW; g). Seawater samples were processed for determination of nutrient concentrations to further derive net flux rates of ammonium, nitrate, nitrite, and phosphate (see method section on "Nutrient analyses").

## Laboratory Incubations of Sponges

To examine whether differences occur in the magnitude and/or the sign between *in-situ* and laboratory sponge incubations, we collected individuals of *V. pourtalesii* (at Sambro Bank Sponge Conservation Area and LaHave Basin), took them to the aquarium room of the Bedford Institute of Oceanography (Dartmouth, Canada) and conducted seven laboratory incubations during a period of 2 weeks, as detailed in Maldonado et al. (2020). The enormous distance from Schulz Bank to any land laboratory made it logistically impossible to repeat the laboratory experiments with the species *S. rosea*.

In short, 11 individuals of *V. pourtalesii* were collected along with the small rock on which it was attached. Sponges were maintained alive on board for 5 days in a 700 L tank filled with seawater refrigerated to 9 ± 1°C. Upon arrival to the laboratory, sponges were transferred to a 360 L tank and left there 2 days for acclimation to a refrigerated (9 ± 0.5°C) seawater system with recirculation, fed with seawater from the Bedford Basin at the head of Halifax Bay. The seawater was filtered on a 1 μm mesh, a pore size preventing phytoplankton but allowing in part of the natural sponge food (i.e., most of the bacterioplankton). After acclimation, each sponge was incubated separately in a polypropylene 16 L container for 24 h and then transferred, along with all other incubated individuals, to a common 300 L water tank for resting during the following 24 h, until starting a new 24 h period of individual incubations in the 16 L containers. The sponges were subjected to a total of seven successive incubations intercalated with their corresponding 24 h resting periods. The idea for this design was to examine whether a midterm exposure to the coastal water in laboratory conditions would induce detectable changes in the sign and magnitude of the net flux of the various nutrients and relative to the field incubations. From each individual incubating container, seawater was sampled at the beginning and at the end of each incubation period to determine the magnitude and the sign of the change in the respective nutrient concentrations (i.e., ammonium, nitrate, nitrite, and phosphate), following the methods explained in the below section of "Nutrient analyses."

## Nutrient Analyses

Immediately after recovering the sampling bottles from deployment, seawater samples were passed through 0.22 μm-pore, syringe filters (Millex-GS Millipore) and frozen at −20°C, until they were analyzed using an Auto-Analyzer AA3 (Bran+Luebbe) following the standard colorimetric method (Strickland and Parsons, 1972), with a determination accuracy of 1%. The nutrient flux was finally calculated as the value of its concentration at the beginning of the incubation minus that at the end of incubation, being normalized by duration of incubation (h), sponge size (mL), and seawater volume in the incubation unit (L) after discounting sponge and rock volume. Flux rates were also corrected by the control flux. Therefore, negative flux values represent nutrient release by the sponges and positive values incorporation. We preferentially expressed data normalized to sponge volume because it facilitates their future applicability to field sponge populations using ROV images without the need of collecting individuals. However, we have also

expressed data as AFDW-normalized, for more correct between-species physiological comparisons. Finally, we examined the potential relationships between flux rates by nutrient pairs and between the flux rate of a nutrient and its ambient concentration at the beginning of the incubation, using linear and non-linear regression analysis.

## Diversity and Functional Gene Analysis of Associated Microbiota

### Microbial Diversity From Amplicon Sequencing

In order to examine the microbial diversity in the studied sponges, 13 individuals of *V. pourtalesii* were collected from Sambro Bank and 13 of *S. rosea* from Schulz Bank. The sample processing procedure is described in detail elsewhere (Busch et al., 2020, 2021; see also these references for data availability). Briefly, from each sponge individual chunks of tissue were subsampled, rinsed and frozen at −80°C until DNA extraction. Seawater reference samples were also collected from each of the two sponge habitats. At Sambro Bank, three samples of bottoms seawater (3 m from bottom) were collected with a Niskin bottle deployed on the ROV. At Schulz Bank, six seawater samples were collected, three of which by Niskin bottles deployed on the ROV (3 m from bottom) and three by a CTD rosette water sampler. All seawater samples (2 L) were filtered onto PVDF filter membranes (Merck Millipore) with a pore size of 0.22 μm and a diameter of 47 mm. Until DNA extraction the filters were stored at −80°C.

Approximately, 0.25 g of sponge tissue and half of a seawater filter were used for DNA extraction with the DNeasy Power Soil Kit (Qiagen). Quality and quantity of extracted DNA was checked and a one-step PCR conducted to amplify the V3 and V4 variable regions of the 16S rRNA gene (primer pair 341F-806R). Afterwards, PCR-products were examined by gel electrophoresis, normalized and pooled. Sequencing was performed on a MiSeq platform (MiSeqFGx, Ilumina) using v3 chemistry (producing 2 × 300 bp).

Adapters were removed and raw sequences (forward reads) were truncated to a length of 270 nt. Quality of sequences was evaluated in QIIME2 version 2018.11 (Bolyen et al., 2019) before applying the DADA2 algorithm (Callahan et al., 2016); one million reads were used to train the error model. Several denoising steps were conducted to remove chimeras, chloroplasts, unassigned and mitochondrial sequences. A minimum sequencing depth of 13000 was applied. Taxonomic classification of Amplicon Sequence Variants (ASVs) was performed using a Bayes classifier (Bokulich et al., 2018) trained on the Silva 132.99% OTUs 16S database (Quast et al., 2013). Between-sample Weighted UniFrac distances (Lozupone et al., 2011) were calculated based on a phylogeny produced with FastTree2 (Price et al., 2010). To assess the effect on Weighted UniFrac distances on the spatial distribution of samples in an ordination space, a non-metric multidimensional scaling (nMDS) was performed, followed by PERMANOVA tests to examine the statistical significance of the between-group differences identified by the nMDS.

### Microbial Functional Gene Repertoire in *V. pourtalesii*

To assess the involvement of microbial symbionts in nitrogen and phosphorous cycling, we focused on the *V. pourtalesii* holobiont. The functional gene repertoire of metagenome-assembled genomes (MAGs) that were used for this objective has been published recently (Bayer et al., 2020) and is available on NCBI under BioProject PRJNA613976. Briefly, metagenomes were sequenced from seven sponge samples and five seawater controls by Illumina Next Generation Sequencing (HiSeq 4000, 2 × 150 bp paired-end) at the Institute of Clinical Molecular Biology (IKMB) of Kiel University. The raw reads were trimmed with Trimmomatic v0.36 and co-assembled with Megahit v1.1.3 (Li et al., 2016). The metagenomic assembly was binned with the metaWRAP pipeline v1.0.2 (Uritskiy et al., 2018), and functionally annotated by Interproscan v5.30-69.0 including GO term and pathway annotations (Jones et al., 2014; Sangrador-Vegas et al., 2016). Interpro annotations are available *via* DOI 10.6084/m9.figshare.12280313. Taxonomy was determined with GTDB-Tk (Chaumeil et al., 2019). *V. pourtalesii*-enriched MAGs were identified by linear discriminant analysis (LDA) scores using LEfSe v1.0 (Segata et al., 2011). For enzymes or functions of specific pathways whose genes were not found in MAGs of identified microbial lineages, we still searched the unbinned metagenomic data (i.e., all contigs not assigned to a specific MAG) to determine whether the genes for the missing metabolic step could be present somehow within the sponge microbial community.

## Histology and Ultrastructure of Deep-Sea Hexactinellids

To understand and document where the various microbes may physically occur within the sponge body, we conducted both light microscopy and transmission electron microscopy (TEM) on *V. pourtalesii* and *S. rosea*.

For light microscopy, tissue pieces of 0.5 $cm^3$ were fixed in 4% formalin in saline dibasic phosphate buffer for 3 weeks, until arriving to the laboratory. Samples were then rinsed in distilled water, desilicified in 5% hydrofluoric acid for 5 h, rinsed in distilled water, dehydrated through an ethanol series of increasing concentration (50–100%) and finally xylene, embedded in paraffin, and sectioned in a Leica RM2125 RTS manual microtome. The obtained 5 μm-thick sections were extended on glass slides, stained with hematoxylin and eosin, and a cover-slide attached using DPX mounting medium for observation through an IX50 Olympus microscope connected to a ProgRes C7 digital camera.

For TEM, tissue pieces of about 2 $mm^3$ were immersed for 3 h in a fixative cocktail consisting of 2% glutaraldehyde, 2% osmium tetroxide, 65% sodium acetate buffer, 11% sucrose, and 20% distilled water (Maldonado, 2015). Initial dehydration steps took place in 50% ethanol and then 70% ethanol, in which samples were preserved for 1 month, until their arrival to the laboratory. Some of these samples were then rehydrated and desilicified in hydrofluoric acid for 5h prior to dehydration; the rest of the samples were subjected to dehydration without desilicification. Dehydration was then resumed in 70% (10 min), 80% (10 min),

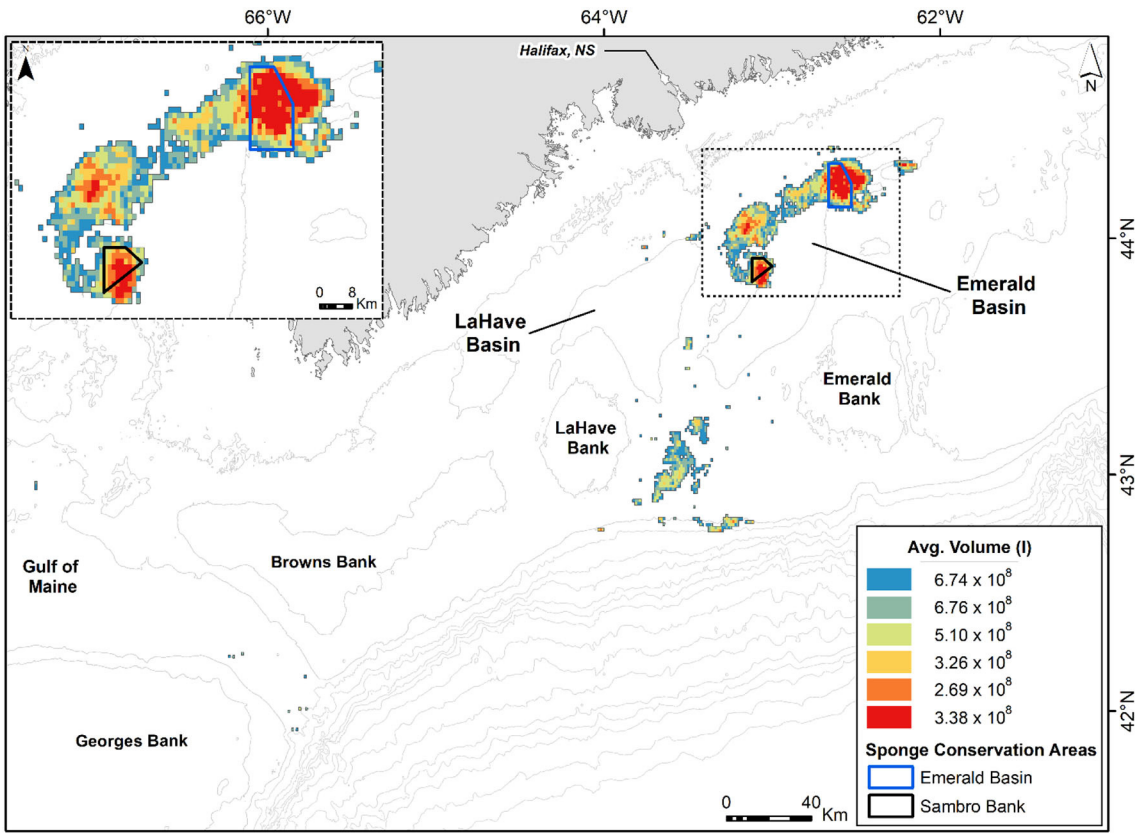


**FIGURE 2 |** Spatial distribution of *Vazella pourtalesii* biomass (by volume in liters) across the Central Scotian Shelf, as calculated in Maldonado et al. (2021). The sponge grounds correspond to areas predicted to have > 70% presence probability of the species, according to Beazley et al. (2018). The areas of densest sponge aggregation are protected from any bottom fishing activity through the creation of two Sponge Conservation Areas (SCA): Emerald Basin SCA and Sambro Bank SCA.

90% (3 × 10 min), 96% (3 × 10 min), and 100% ethanol (3 × 10 min), followed by propylene oxide (2 × 10 min). Embedding in Spur resin required five immersion steps with gentle shaking during each one: 6 h in a 3:1 propylene-oxide/resin solution, 12 h in 2:2 propylene-oxide/resin solution, 7 h in a 1:3 propylene-oxide/resin solution and two 6-h steps in pure resin. Resin was hardened at 60°C for 2 days. Ultrathin sections were obtained with an Ultracut Reichert-Jung ultramicrotome, mounted on gold grids and stained with 2% uranyl acetate for 30 min, then with lead citrate for 10 min. Observations were conducted with a JEOL 1010 TEM operating at 80 kv and provided with an external Gatan module for acquisition of digital images.

## Nutrient Fluxes at the Deep-Sea Community Level

The nutrient utilization rates measured during the *in-situ* and laboratory incubations were used to estimate the net annual flux of ammonium, nitrite, nitrate, and phosphate at the aggregation of *V. pourtalesii*, which is well-characterized in terms of the spatial distribution of the sponge biomass. The area occupied by the *Vazella* sponge grounds on the Scotian Shelf was estimated by applying a threshold criterion (70%) to the modeled presence probability outputs for this species, as indicated in Beazley et al. (2018). The presence probability surface was generated from random forest modeling using presence/absence data. Using ArcMap version 10.6.1., the 1 × 1 km raster grid containing all predicted presence probabilities of *V. pourtalesii* from > 70 to 100% and displayed in 5% equal presence probability intervals in Beazley et al. (2018), was converted to a polygon layer of 1 × 1 km cells, each representing a given presence probability. The total area encompassed by all cells with probability values within each 5% probability interval (six intervals from > 70 to 100%) was calculated at 2,105 $km^2$ (**Figure 2**). The two densest areas of the sponge aggregation were closed by Fisheries and Oceans Canada to all bottom fishing activities, creating in 2013 the Emerald Basin Sponge Conservation Area (195 $km^2$) and the Sambro Bank Sponge Conservation Area (62 $km^2$), as indicated in **Figure 2**. ROV-driven, transect and quadrat surveys in the two Sponge Conservation Areas additionally characterized the spatial distribution of both the individuals (i.e., density) and the individual biomass (in volume) in cells of highest presence probability, as detailed in Maldonado et al. (2021). It was found that, at the densest areas of the aggregations (cells of 0.975 presence probability), the sponge density was 3.78 ± 3.22 individuals $m^{-2}$, with a biomass of 1.6 ± 2.8 L of sponge tissue

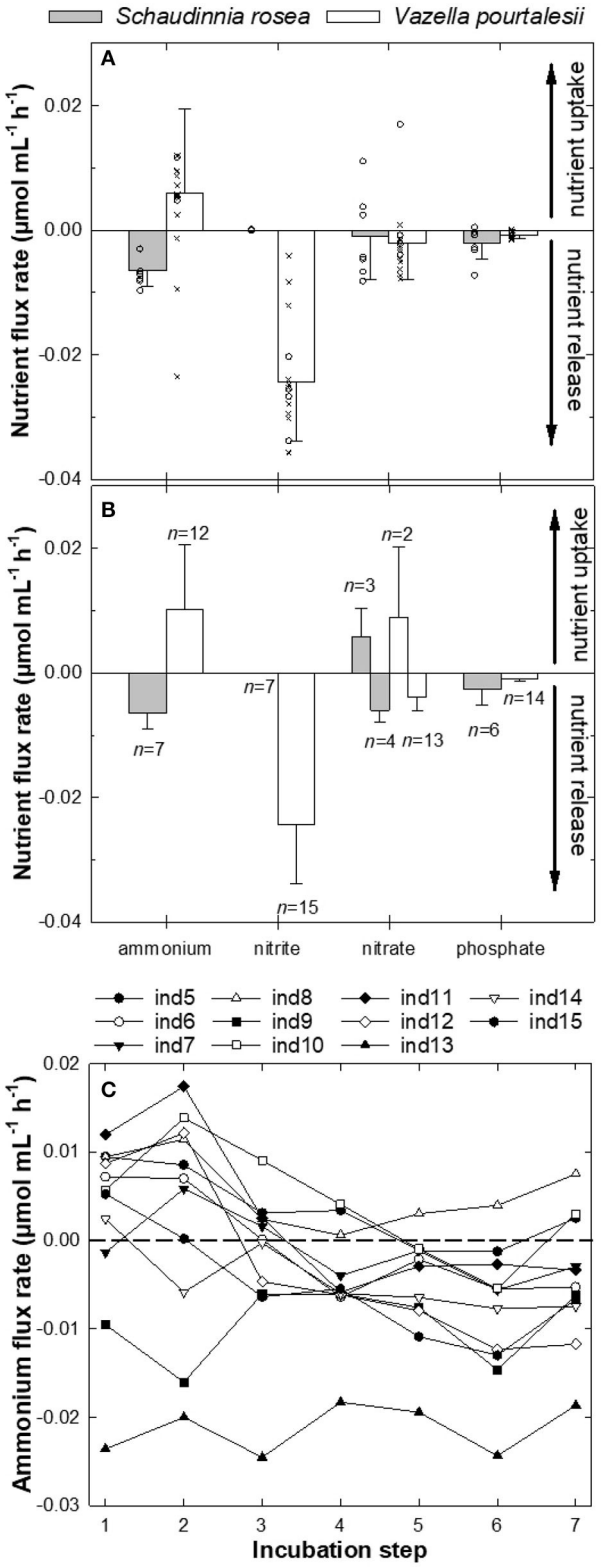


**FIGURE 3 | (A,B)** Magnitude (average ±SD) and sign of the flux (µmol $mL^{-1}$ $h^{-1}$) of ammonium ($NH_4^+$), nitrite ($NO_2^-$), nitrate ($NO_3^-$), and phosphate ($PO_4^{3-}$) measured for individuals of the hexactinellid sponges *Schaudinnia rosea* and *Vazella pourtalesii*. Note that positive values indicate incorporation of a nutrient from the seawater into the sponge, while negative values indicate nutrient release from the sponge. **(A)** Global average (±SD) flux rate (µmol $mL^{-1}$ $h^{-1}$) for each nutrient and sponge species when all assayed individuals are considered in the calculations (*S. rosea, n* = 7; *V. pourtalesii, n* = 15). Note that individual measurements for *in-situ* incubations (crosses) and the first laboratory incubation of *V. pourtalesii* (open circles) are also plotted to show between individual variability. **(B)** Average (±SD) flux rates (µmol $mL^{-1}$ $h^{-1}$) considering only individuals with the same flux sign in the averaging process. The number of individuals (*n*) considered in these averages by flux sign for each nutrient and species are indicated in the graph. **(C)** Ammonium flux rate in the *V. pourtalesii* individuals over the seven successive laboratory incubations. See **Supplementary Table 2** for ammonium concentration at the onset of incubations.

*(Continued)*

$m^{-2}$. Finally, in order to convert presence probability into density of sponges and sponge biomass, as required for successively estimating the flux rate of the respective dissolved inorganic nutrient across the *Vazella* grounds, the average sponge density and volume of sponge tissue were respectively multiplied by the mid-point of each 5% presence probability bin. This procedure revealed that the aggregation consists of some 6,479 ± 5,518 million sponges, with a total sponge biomass (in volume) of 2,791 ± 3,832 million L (Maldonado et al., 2021). The biomass is known to be spatially distributed on the Nova Scotia Central Shelf, as it is indicated in **Figure 2**. The resulting spatial cells of sponge biomass were then multiplied by the global average value of the net flux rate obtained for each nutrient after combining all individuals from *in-situ* and laboratory incubations. For the laboratory net flux, the average values considered only the first incubation of the individuals. By considering only the first laboratory incubation, we had more chances of avoiding the effects that the coastal seawater feeding the laboratory could have on the microbiota of *V. pourtalesii,* minimizing physiological artifacts in the sponge response. Indeed, to test whether the results of "*in-situ*" and "first-day laboratory" incubations could be pooled safely, we examined potential differences in the net flux rate between *in-situ* incubations and the first-day laboratory incubations for each nutrient, using either the *t*-test or its non-parametric equivalent Mann-Whitney *U*-test, whenever required to deal with non-normal and/or heteroscedastic data sets. In all cases, there were no statistically significant differences between *in-situ* and laboratory flux rates (see **Supplementary Table 1**) and, consequently, data were suitable for pooling. The result of the subsequent calculations provided a mean (± SD) estimate of the annual net flux rate of each nutrient through the *V. pourtalesii* aggregations on the Nova Scotia Continental Shelf.

It must be noted that the large standard deviations associated to the average values of number of sponges per square meter, volume of sponge per square meter, and total number of individuals in the aggregation obtained from Maldonado et al. (2021), when propagated through the scaling up of data to the aggregation level, will lead to a large SD value associated to the average of the global fluxes. As explained in Maldonado et al. (2021), the large SD values of sponge density and volume initially derive from the largest individuals of *V. pourtalesii* being often connected by their bases, forming small clumps of individuals. As a result, even within the most densely populated areas of the

aggregation, some square meters of bottom are devoid of sponges while others contain many. Such spatial pattern, aggregated at a scale $<1$ m$^2$, does not affect the accuracy and reliability of the average values derived for the entire extension of the sponge aggregation despite increasing their SD.

# RESULTS

## Nutrient Flux Rates of Sponges

The two assayed species showed different patterns in the sign of ammonium flux, despite the fact that they were exposed to nearly identical ambient concentrations of this nutrient during the incubations ($1.18 \pm 1.13$ μM for *S. rosea* and $1.23 \pm 0.66$ μM for *V. pourtalesii*). All assayed individuals of *S. rosea* were net sources of ammonium in their natural habitat. Individual efflux rate ranged from $-3.0$ to $-9.7 \times 10^{-3}$ μmol mL$^{-1}$ h$^{-1}$, with an average rate of $-6.5 \pm 2.6 \times 10^{-3}$ μmol mL$^{-1}$ h$^{-1}$ (**Figures 3A,B**, **Table 1**). In contrast, all *V. pourtalesii* incubated *in situ* (**Figure 3A**, **Table 2**: individuals 1–4) were net ammonium sinks ($15.8 \pm 17.4 \times 10^{-3}$ μmol mL$^{-1}$ h$^{-1}$). During the first laboratory incubation, most of the 11 assayed individuals of *V. pourtalesii* were also net ammonium sinks, except for individuals #7, #9, and #13, which released this nutrient at a rate of $-1.4$, $-9.5$, and $-23.6 \times 10^{-3}$ μmol mL$^{-1}$ h$^{-1}$, respectively (**Figures 3A,B**, **Table 2**, **Supplementary Table 2**). Pairwise tests revealed no statistically significant difference in the average flux rate of ammonium (neither in the rest of nutrients) when measured *in situ* or during the 1st day of laboratory incubations (**Supplementary Table 1**). Therefore, flux rates from *in-situ* and laboratory incubation were pooled, yielding an average rate of ammonium consumption by *V. pourtalesii* of $5.9 \pm 13.5 \times 10^{-3}$ μmol mL$^{-1}$ h$^{-1}$ (**Figure 3A**, **Table 2**). However, it was surprising that after the first laboratory incubation, the ammonium flux started changing in most individuals, which shifted toward net ammonium sources after the third day of incubation and persisted in that condition for the following 4 incubations, to the end of the experiment (**Figure 3C**, **Table 2**, **Supplementary Table 2**). This shift suggests that changes in the population of associated microbes responsible for the ammonium are happening, even if only a few days after the sponges were moved from their natural habitats (see Discussion). Similar shifts in the flux rate of nitrite, nitrate, and phosphate did not occur.

Regarding nitrite, the assayed individuals of *S. rosea* showed insignificant flux rates close to zero that fell below the detection limits of the analysis and, therefore, these sponges cannot be defined as either sinks or sources of nitrite from our incubation approach (**Figure 3**, **Table 1**). In contrast, all *V. pourtalesii* released nitrite during both *in-situ* and laboratory incubations. The nitrite concentration in the sponge habitat was $0.12 \pm 0.06$ μM and the nitrite release rate during the *in-situ* incubations averaged $-26.6 \pm 5.6 \times 10^{-3}$ μmol mL$^{-1}$ h$^{-1}$ (**Table 2**). The nitrite concentration in the laboratory water was higher ($2.22 \pm 0.07$ μM) than in the natural sponge habitat and the average rate of nitrite release in the laboratory incubation was only slightly smaller than that in field conditions, $-23.4 \pm 10.7 \times 10^{-3}$ μmol mL$^{-1}$ h$^{-1}$ (**Table 2**).

The nitrate flux reflected marked inter-individual differences in both its magnitude and sign, obscuring the identification of a consistent pattern in any of the two assayed species (**Figure 3**). In the natural habitat of *S. rosea*, nitrate concentration was $14.55 \pm 0.94$ μM. In those conditions, four of the *in-situ* incubated individuals released nitrate at an average rate of $-6.0 \pm 1.8 \times 10^{-3}$ μmol mL$^{-1}$ h$^{-1}$ and three others consumed nitrate at a similar average rate, $5.7 \pm 4.7 \times 10^{-3}$ μmol mL$^{-1}$ h$^{-1}$ (**Figure 3**, **Table 1**). In the case of *V. pourtalesii*, 3 of the 4 *in-situ* incubated individuals, at natural nitrate concentrations of $17.21 \pm 1.56$ μM, were net sources of nitrate, with a rate of $-3.8 \pm 2.3 \times 10^{-3}$ μmol mL$^{-1}$ h$^{-1}$. Likewise, most individuals incubated in the laboratory —at the nitrate concentration $7.86 \pm 0.15$ μM characterizing the laboratory seawater— were also net nitrate sources, rendering a collective average efflux rate of $-3.8 \pm 2.3 \times 10^{-3}$ μmol mL$^{-1}$ h$^{-1}$. Among the net nitrate consumers there was individual #2, which consumed nitrate during the *in-situ* incubation at a rate

**TABLE 1 |** Flux of nutrients measured through *in-situ* incubations of *Schaudinnia rosea*.

| Code | *Size* (*mL*) | Initial nutrient concentration (μM) | | | | Nutrient flux rate ($10^{-3}$ μmol mL$^{-1}$ h$^{-1}$) | | | |
|---|---|---|---|---|---|---|---|---|---|
| | | $NH_4^+$ | $NO_2^-$ | $NO_3^-$ | $PO_4^{3-}$ | $NH_4^+$ | $NO_2^-$ | $NO_3^-$ | $PO_4^{3-}$ |
| 1 | 114.8 | 1.75 | 0.04 | 14.15 | 0.91 | −8.2 | 0.0 | −6.7 | −7.3 |
| 2 | 287.5 | 3.29 | 0.05 | 14.50 | 0.67 | −3.0 | 0.0 | 11.0 | 0.5 |
| 3 | 143.6 | 1.61 | 0.06 | 14.06 | 0.79 | −9.7 | 0.1 | −4.3 | −2.8 |
| 4 | 168.8 | 0.18 | 0.06 | 13.80 | 0.90 | −7.1 | 0.0 | −4.7 | −0.8 |
| 5 | 258.7 | 0.23 | 0.03 | 14.04 | 0.87 | −3.0 | 0.0 | −8.2 | −0.8 |
| 6 | 120.0 | 0.72 | 0.04 | 14.73 | 0.91 | −6.6 | 0.0 | 3.7 | −0.4 |
| 7 | 270.0 | 0.47 | 0.04 | 16.57 | 0.99 | −7.8 | −0.1 | 2.4 | −3.2 |
| AVG | 194.8 | 1.18 | 0.05 | 14.55 | 0.86 | −6.5 | 0.0 | −1.0 | −2.1 |
| SD | 74.8 | 1.13 | 0.01 | 0.94 | 0.10 | 2.6 | 0.1 | 6.9 | 2.6 |

*Seven individuals were incubated (code), their size (mL) determined, and the initial concentration of nutrients (ammonium: $NH_4^+$; nitrite: $NO_2^-$; nitrate: $NO_3^-$; phosphate: $PO_4^{3-}$) in the chamber measured, along with the detected nutrient flux rate ($10^{-3}$ μmol per hour and mL of sponge tissue). Nutrient flux rates were corrected by the control effect. The average (AVG) and standard deviation (SD) of the set of individual measurements are given in the bottom rows.*

**TABLE 2 |** Summary of nutrient fluxes and associated parameters in the incubations of *Vazella pourtalesii*.

| Code | Size (mL) | Initial nutrient concentration (μM) | | | | | | Nutrient flux rate ($10^{-3}$ μmol mL$^{-1}$ h$^{-1}$) | | | | | |
|---|---|---|---|---|---|---|---|---|---|---|---|---|---|
| | | $NH_4^+$ | | | $NO_2^-$ | $NO_3^-$ | $PO_4^{3-}$ | $NH_4^+$ | | | $NO_2^-$ | $NO_3^-$ | $PO_4^{3-}$ |
| | | 1st | 1st-3th | 4–7th | | | | 1st | 1st-3th | 4–7th | | | |
| 1 | 492.4 | 0.04 | – | – | 0.14 | 15.66 | 1.08 | 5.3 | – | – | −25.5 | −4.0 | −0.9 |
| 2 | 64.5 | 0.12 | – | – | 0.05 | 17.35 | 1.14 | 41.6 | – | – | −33.8 | 17.0 | −0.4 |
| 3 | 126.4 | 0.08 | – | – | 0.09 | 16.51 | 1.11 | 11.7 | – | – | −20.3 | −0.8 | −0.5 |
| 4 | 323.4 | 0.56 | – | – | 0.19 | 19.31 | 1.26 | 4.7 | – | – | −26.7 | −2.2 | −1.0 |
| 5 | 65.2 | 1.52 | 1.71 | 0.68 | 2.13 | 7.91 | 0.96 | 9.4 | 7.0 | 0.9 | −30.2 | −2.8 | −0.3 |
| 6 | 144.3 | 1.57 | 1.73 | 0.81 | 2.25 | 7.84 | 0.97 | 7.2 | 4.7 | −4.8 | −29.5 | −4.6 | −0.3 |
| 7 | 104.8 | 1.62 | 1.84 | 0.74 | 2.20 | 7.72 | 0.95 | −1.4 | 2.0 | −3.4 | −24.8 | −7.9 | −1.5 |
| 8 | 108.4 | 1.55 | 1.58 | 0.64 | 2.22 | 7.73 | 0.96 | 9.4 | 7.7 | 3.8 | −35.8 | −6.3 | −1.4 |
| 9 | 50.8 | 1.64 | 1.76 | 0.74 | 2.14 | 8.01 | 0.95 | −9.5 | −10.5 | −8.6 | −12.1 | −3.1 | −1.3 |
| 10 | 58.0 | 1.78 | 1.76 | 0.69 | 2.21 | 7.89 | 0.91 | 5.7 | 9.5 | 0.2 | −28.0 | 0.8 | 0.1 |
| 11 | 86.8 | 1.56 | 1.69 | 0.75 | 2.40 | 8.19 | 0.97 | 11.9 | 10.6 | −3.7 | −35.7 | −7.3 | −1.3 |
| 12 | 65.2 | 1.58 | 1.70 | 0.72 | 2.20 | 7.85 | 0.96 | 8.7 | 5.4 | −9.6 | −24.0 | −5.1 | −0.9 |
| 13 | 36.5 | 1.58 | 1.80 | 0.70 | 2.19 | 7.88 | 0.99 | −23.6 | −22.7 | −20.2 | −4.1 | −1.4 | −0.2 |
| 14 | 65.2 | 1.66 | 1.77 | 0.68 | 2.21 | 7.81 | 0.95 | 2.4 | −1.2 | −6.9 | −25.3 | −2.4 | −1.6 |
| 15 | 43.6 | 1.59 | 1.80 | 0.76 | 2.22 | 7.64 | 0.99 | 5.2 | −0.3 | −9.0 | −8.4 | −1.7 | −1.0 |
| AVG | 122.4 | 1.23 | 1.74 | 0.72 | 1.66 | 10.35 | 1.01 | 5.9 | 1.1 | −5.6 | −24.3 | −2.1 | −0.8 |
| SD | 124.1 | 0.66 | 0.07 | 0.05 | 0.96 | 4.34 | 0.09 | 13.5 | 9.9 | 6.5 | 9.5 | 5.8 | 0.5 |

*The table contains reference labels for the 15 incubated individuals, with individuals #1 to #4 corresponding to in-situ incubations and individuals #5 to #15 corresponding to laboratory incubations. It is also given the size of the incubated sponges, the initial concentration (μM) of the dissolved inorganic nutrients (ammonium: $NH4^+$; nitrate: $NO3^-$; nitrite: $NO2^-$; phosphate—$PO_4^{3-}$) at each incubation event, and the nutrient flux rate ($10^{-3}$ μmol mL$^{-1}$ h$^{-1}$) detected during the incubation and normalized by incubation duration and sponge biomass. Nutrient flux rates have also been corrected for the control effect. Note that for the laboratory ammonium flux rate, data are presented for only the 1st day of laboratory incubations (1st), then as the individual responses averaged across the first three laboratory incubations (1st–3th), then as the individual responses averaged across the last four laboratory incubations (4th–7th). See also* ***Supplementary Table 2*** *for raw data on ammonium flux rate across all laboratory incubations. The global average (AVG) and standard deviation (SD) of the various parameters for the entire set of assayed individuals are summarized at the two bottom rows of the table.*

of $17.0 \times 10^{-3}$ μmol mL$^{-1}$ h$^{-1}$; individual #10 also consumed nitrate during the laboratory incubations, but at much smaller rate of $0.8 \times 10^{-3}$ μmol mL$^{-1}$ h$^{-1}$ (**Table 2**).

Regarding phosphate, both species were predominantly net sources, but with low rates. Natural phosphate concentration during the *in-situ* incubations of *S. rosea* was 0.86 ± 0.10 μM (**Table 1**). At that nutrient concentration, 6 of the 7 assayed individuals released phosphate, with an average rate of $-2.5 \pm 2.6 \times 10^{-3}$ μmol mL$^{-1}$ h$^{-1}$ (**Figure 3**). In contrast, individual #2 consumed phosphate at a low rate of $0.5 \times 10^{-3}$ μmol mL$^{-1}$ h$^{-1}$ (**Table 1**). All four individuals of *V. pourtalesii* incubated *in situ* under a natural phosphate concentration of 1.15 ± 0.08 μM released phosphate at an average rate of $-0.7 \pm 0.3$ x $10^{-3}$ μmol mL$^{-1}$ h$^{-1}$. Ten of the 11 individuals incubated in the laboratory at a phosphate concentration of 0.96 ± 0.02, that is, similar to the one in the natural habitat, also released phosphate consistently, with an average rate of $-1.0 \pm 0.5 \times 10^{-3}$ μmol mL$^{-1}$ h$^{-1}$ (**Figure 3**). Individual #10 consumed phosphate at a rate as low as $0.1 \times 10^{-3}$ μmol mL$^{-1}$ h$^{-1}$ (**Table 2**), so that it cannot be discarded that it was indeed inactive in terms of release and that the sign of the flux is an artifact derived from the flux rates being at the limit of the methodological detection.

When the relationship between flux rates was examined by pairs of nutrients using both linear and non-linear regression analyses, no statistically significant relationships were found for *S. rosea* in any case ($n = 7$, $p > 0.05$). In contrast, statistically significant relationships, although of only moderate intensity, were found in *V. pourtalesii* (**Figure 4**). It was detected that the increase in the release rate of nitrite is linearly coupled to an increase in the ammonium consumption ($n = 15$, $R^2 = 0.474$, $p = 0.005$; **Figure 4A**). Another detected relationship was that the rate of nitrate consumption decreased linearly with the increase of phosphate release ($n = 14$, $R^2 = 0.379$, $p = 0.019$; **Figure 4B**).

When the relationship between the flux rate of a nutrient and its ambient concentration was examined by linear regression, no statistical significance was found for any of the nutrients in any of the two sponge species (**Supplementary Figure 1**).

## Microbial Insights Into the Sponge Nitrogen Flux

The analysis of amplicon sequences sampled from *V. pourtalesii* and *S. rosea* showed that each species harbors a distinct microbiome (**Figure 5**, **Supplementary Table 3**, **Supplementary Data File 1**). In each case, there are also statistically significant differences between the sponge microbiome and that of the surrounding seawater. Microbiome differences between *V. pourtalesii* and *S. rosea* may be responsible for some of the between-species differences detected in the sign

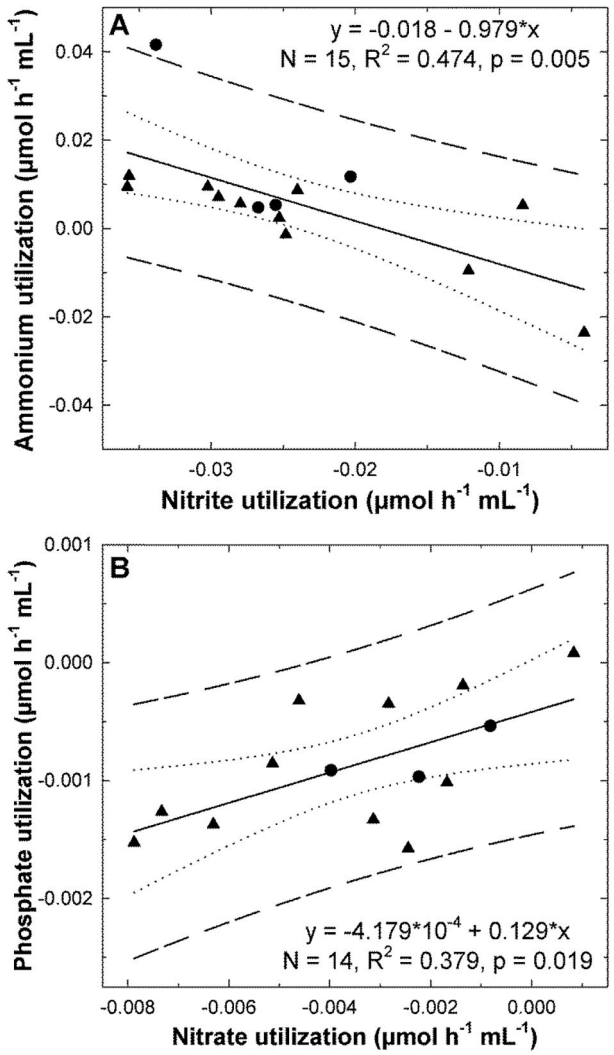


**FIGURE 4 |** Significant relationships between nutrient fluxes in *Vazella pourtalesii*. **(A)** The lower the rate of nitrite release, the higher the ammonium consumption. **(B)** When individual #2, an atypical outlier consuming nitrate at the abnormally high rate of 17 nmol $mL^{-1}$ $h^{-1}$ —rather than releasing it–, was excluded from the analysis, a linear significant relationship was revealed between the release rates of nitrate and phosphate. The rest of possible pairwise combinations among the flux rates of all four nutrients were also examined, but none had statistically significant support.

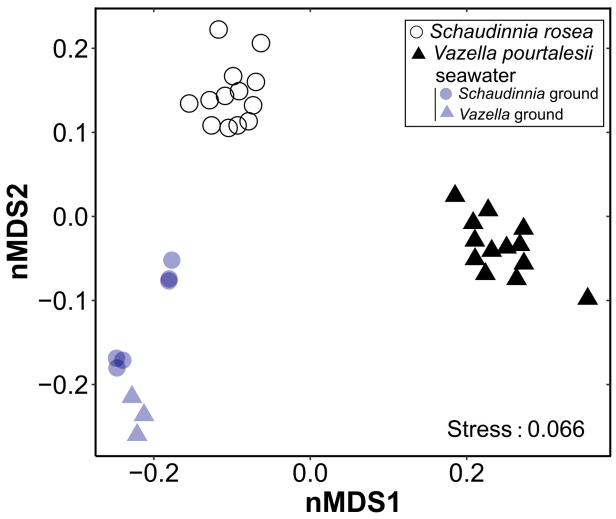


**FIGURE 5 |** Non-metric dimensional scaling (nMDS; $k = 2$, maxit = 100) plot on weighted UniFrac distances for each of the assayed sponge species, *Vazella pourtalesii* and *Schaudinnia rosea*, and the seawater of their respective habitats. The results of the PERMANOVA tests that gives statistical support to the between-group differences is given in **Supplementary Table 3**.

and magnitude of the flux of the various nutrients (**Figures 3A,B**, **Tables 1**, **2**).

## Microbes of the Nitrogen Cycle in *V. pourtalesii*

We evaluated the potential metabolic functions of *V. pourtalesii*-associated microbes involved in the nitrogen cycle by searching for key enzymes in the MAGs, which allows the assignment of function to members of the microbiome. For enzymes or functions encoded on contigs that were not sorted into specific MAGs, we assumed that the function might be present in the microbial community (**Supplementary Table 4**). Genes involved in nitrification, denitrification, dissimilatory nitrate reduction, nitrogen fixation and ammonia assimilation were identified. Genes encoding for anammox or assimilatory nitrate reduction were found neither in MAGs nor in the unbinned metagenomic data.

### *Nitrification*

The enzyme ammonia-monooxygenase (AMO), responsible for the first reaction in the first step of nitrification (i.e., oxidation of ammonia to hydroxylamine), was detected in the Nitrosopumilaceae (Crenarchaeota, MAGs 74, 90, 131, 143) and in the Nitrosomonadaceae (Proteobacteria, MAG 46). This microbial metabolism may contribute to explain why most individuals of *V. pourtalesii* were essentially net consumers of ammonium. After 3 incubation steps in the laboratory using coastal water, all *V. pourtalesii* individuals became net sources of ammonium. Thus, we cannot discard the possibility that the Nitrosopumilaceae and Nitrosomonadaceae populations decayed in laboratory seawater because being highly dependent on the seawater/holobiont conditions of the natural habitat (see Discussion). Interestingly, the MAGs enriched in *V. pourtalesii* compared to seawater (**Supplementary Table 4**, **Supplementary Data File 2**) include the genus *Cenarchaeum* (MAGs 74, 90, 143), which is a common sponge-specific AOA symbiont. MAG 131 was found in equal abundances in both habitats and represents the genus *Nitrosopumilus*, a common sea-water AOA. The hydroxylamine-oxidoreductase (HAO), responsible for the second reaction in the first step of nitrification converting hydroxylamine to nitric oxide that is subsequently converted to nitrite by a not yet identified enzyme (Caranto and Lancaster, 2017), was not detected in

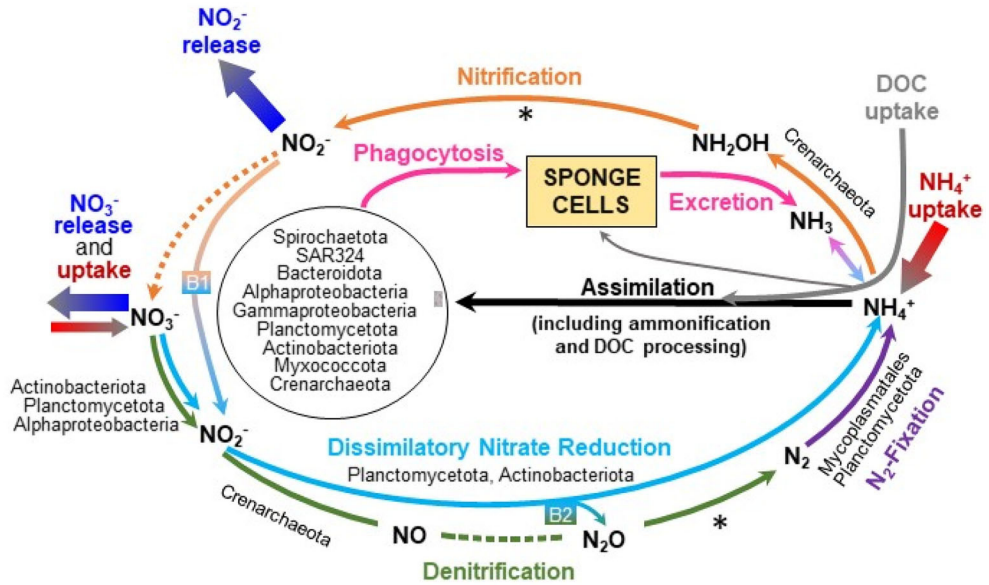


**FIGURE 6 |** Graphical summary of the microbiome-driven nitrogen cycle in *Vazella pourtalesii,* as it has been deduced through the metagenomic study and the incubation experiments. Note that only those N pathways for which MAGs were found to be enriched in the sponge are named in the graph. The dashed lines indicate enzymatic pathways for which genes were not detected and the asterisk (*) indicates genes that were present only in the unbinned data. "B1" and "B2" refer to putative bridges between major biochemical pathways, which provide alternative routes to palliate the effects of some missing enzymes, also allowing an efficient closing of the N cycle in the holobiont. The N microbial engine of *V. pourtalesii* appears to revolve around the incorporation of ammonium from the seawater and its internal recycling. This nutrient fosters N assimilation by the sponge microbiota, which also benefits from the important amounts of DOC taken up by the sponge. All available evidence suggests that the nourishment of *V. pourtalesii* does not appear to be based on filter feeding of the free-living bacterioplankton but rather on the phagocytosis of its internal microbiota, which is mostly farmed in the bacteriosyncytia through the supply of ammonium and DOC.

the MAGs. However, *haoB*-related genes were found in the unbinned metagenome data, suggesting that this enzyme may be present in at least some of the microbial lineages and that nitrite is produced out of ammonia/ammonium. Genes responsible for nitrite oxidation, the second step of nitrification, were found neither in MAGs nor in the unbinned metagenomic data. The lack of those enzymes would explain why nitrite, which appears not to be further processed in the nitrification pathway (**Figure 6**), is released at high rate by *V. pourtalesii* (**Figure 3**, **Table 2**, **Supplementary Tables 1, 2**). The occurrence of ammonia oxidation activity in the absence of nitrite oxidation was in agreement with the finding that ammonium consumption and nitrite release are activities associated with statistical significance in *V. pourtalesii* (**Figure 4A**).

### *Denitrification*

Genes encoding enzymes involved in two of the four reactions of the denitrification pathway were found in the microbiome of *V. pourtalesii.* Genes annotated as nitrate reductase, which catalyze the reduction of nitrate to nitrite, were found in three MAGs (**Supplementary Table 4**) assigned to Alphaproteobacteria (MAG 70), Actinobacteria (MAG 64), and Planctomycetota (MAG 52). All three MAGs were enriched in the sponge compared to seawater. Yet, the sources of nitrate to initially feed denitrification remain unclear, since nitrification cannot be completed in *V. pourtalesii* and external nitrate was not consistently incorporated from seawater by all assayed individuals, only a minority of them being net nitrate consumers (**Figures 3**, **6**, **Table 2**). The genes *nirS and nirK* encoding the nitrite reductase that catalyzes the conversion of nitrite into nitric oxide were detected in five MAGs belonging to Crenarchaeota (MAGs 36, 90, 101, 131, 143) and in the acidobacterial MAG 86. The MAGs 90 and 143 were enriched in *V. pourtalesii* over seawater. Regarding the last two reactions of denitrification that lead to production of molecular $N_2$ gas, we could not detect the genes encoding for the nitric oxide reductase and nitrous-oxide reductase enzymes in the MAGs, but the gene for the latter was present in the unbinned data (**Figure 6**). Given that nitrite is accumulated by an incomplete nitrification and released by the sponges at relatively high rates (**Figure 3**), it cannot be discarded that part of the accumulated nitrite can be used to feed the denitrification pathway at its intermediate step (**Figure 6**) and also the pathway of dissimilatory nitrate reduction to ammonium, as it is explained in the section below.

### *Dissimilatory Nitrate Reduction to Ammonium (DNRA)*

We detected genes involved in DNRA, which is an important intermediate process in the N cycling, linking N-compound oxidation and reduction processes, that is, operating at the oxic-anoxic interface. Genes coding for nitrate reductase —which may operate not only in the DNRA pathway but also in the previously described denitrification pathway— were found in three MAGs (**Supplementary Table 4**) of Alphaproteobacteria (MAG 70), Actinobacteria (MAG 64), and Planctomycetota

(MAG 52). All three MAGs were enriched in the sponge compared to seawater. The second step in the dissimilatory reduction to ammonium is mediated by two enzymes. One is a respiratory cytochrome c nitrite reductase, encoded by genes *nrfA/ H,* which was detected only in the unbinned metagenomic data (**Supplementary Table 4**). The other is a NADH depended nitrite reductase encoded by the genes *nirB/ D*, detected in four MAGs affiliated with Planctomycetota (MAGs 52, 99), Actinobacteria (MAG 64), and Gammaproteobacteria (MAG 89), although the latter was not significantly enriched in *V. pourtalesii* over seawater. These features agree with the idea that the holobiont metabolism of *V. pourtalesii,* in its natural habitat, tends to produce internally ammonia/ammonium, which appears to be subsequently used as a preferred substrate to sustain the populations of archaea and bacteria of the microbiota (**Figure 6**). Note that only some of the assayed individuals of *V. pourtalesii* incorporated nitrate from seawater (**Figures 3**, **6**). Therefore, it is assumed that the DNRA pathway is mostly fed with nitrite at an intermediate step, using for that purpose part of the nitrate accumulated after the incomplete nitrification (**Figure 6,** B1 arrow). This bridging mechanism is relevant because it connects the aerobic process of nitrification to the anaerobic process of DNRA and it would provide an explanation of the withstanding of *V. pourtalesii* to low oxygen conditions.

### *Nitrogen Fixation*

Genes for nitrogenase enzymes involved in N fixation through reduction of $N_2$ gas to $NH_4^+$ were detected in several MAGs (**Figure 6**, **Supplementary Table 4**) affiliated with Firmicutes (MAGs 77, 88, 127), Planctomycetota (MAG 91), Bacteroidota (MAG 24), and Alphaproteobacteria (MAG 135). The MAGs 88 and 91 were enriched in *V. pourtalesii* over seawater. Note that if the incomplete denitrification process previously identified in *V. pourtalesii* can be completed somehow by the sponge microbiome (see Discussion from bridging between DNRA and denitrification), the resulting $N_2$ could well provide substratum for this N-fixation pathway (**Figure 6**).

### *Ammonia Assimilation*

The enzymes glutamine synthetase (*glnA, GLUL*) and glutamate dehydrogenase (*gudB, rocG*) were found in the MAGs of several members of the *V. pourtalesii*-microbiota (**Supplementary Table 4**), indicating that amino acids can be formed from ammonia. MAGs enriched in *V. pourtalesii* were affiliated with the phyla Alpha- and Gammaproteobacteria, Spirochaetota, Crenarchaeota, Planctomycetota, SAR324, Actinobacteriota, and Verrucomicrobiota (**Figure 6**; **Supplementary Table 4**, **Supplementary Data File 2**). Again, these findings support the notion that the pool of ammonium within the sponge, which consists of the ammonium excreted by the sponge cells (i.e., ammonia that undergoes molecular auto-ionization to ammonium and amide ions) plus that produced by the denitrification and DNRA pathways and that taken up from seawater, serves as a preferred substratum to sustain the growth of the bulk of the microbiota in *V. pourtalesii*.

## Identification of Genes and Microorganisms of the Phosphorus Cycle

We searched for enzymes involved in the phosphorous cycle in the annotation data derived from the *V. pourtalesii* microbiome to elucidate which members might be responsible for the low but consistent release of phosphate detected in the sponges (**Figure 3**, **Table 1**). Components of the C–P lyase multienzyme complex were found (**Supplementary Table 4**, **Supplementary Data File 2**). This complex is encoded by 14 genes (*phnCDE, phnF, phnGHIJKLM*) and catalyzes the dephosphonation reaction in a range of structurally diverse phosphonates, that is, organophosphorus compounds containing C-PO(O*X*)$_2$ groups, where "*X*" is either H or an alkyl or aryl radical. Phosphonates are one of the sources of phosphate intake into cells. The dephosphonation reaction by biological vias (i.e., enzymatically) is physiologically relevant because the C-P bond is extremely stable and its cleavage by chemical vies requires very aggressive conditions. Enzyme subunits of the C–P lyase complex were found only in MAG 124 belonging to Alphaproteobacteria, but the detection in the unbinned data suggests that more members in the microbiome may be using this enzyme for phosphonate utilization. This assumption is supported by the detection of subunits of the ABC transporter in several MAGs representing different phylogenetic groups (**Supplementary Table 4**). The predominant biogenic orthophosphate in nature is 2-Aminoethylphosphonate (2AEP) and its utilization is a two-step process. The first step is the transamination of 2AEP (+ pyruvic acid) to 2-phosphoacetaldehyde (PAA) and L-alanine (Ternan et al., 1998). This enzyme was found in several MAGs (**Supplementary Table 4**) of which members of Planctomycetota (MAGs 52, 94, 116, 119), Crenarchaeota (MAGs 74, 90, 143), Alphaproteobacteria (MAG 75), and Gammaproteobacteria (MAG 10) were enriched in the sponge. The second step is the hydrolytic cleavage of PAA in phosphate and acetaldehyde mediated by the enzyme phosphonoacetaldehyde hydrolase. This was found only in two *V. pourtalesii*-enriched MAGs (52, 119) representing Planctomycetota.

The enzyme phosphonoacetate hydrolase is a alkaline phosphatase, cleaving C-P bounds of a given substrate to form acetate and phosphate (reviewed in Villarreal-Chiu et al., 2012). This was found in one *V. pourtalesii*-enriched member of Planctomycetota (MAG 121) and in several MAGs of different phylogenetic groups (**Supplementary Table 4**). Collectively, the results suggest that part of the sponge microbiota use phosphonates as a source of phosphorous to grow and, through this activity, the sponge gets help in the hard task of degrading phosphonates. The level at which this process explains the net phosphate efflux from the sponges remain unclear from our approach and more research is needed to better understand the P circuit in the holobiont.

## Ultrastructural Observations

The histological study of *S. rosea* and *V. pourtalesii* indicated that the tissue in these hexactinellids is a delicate network of thin strands through which the large silica pieces of the skeleton and

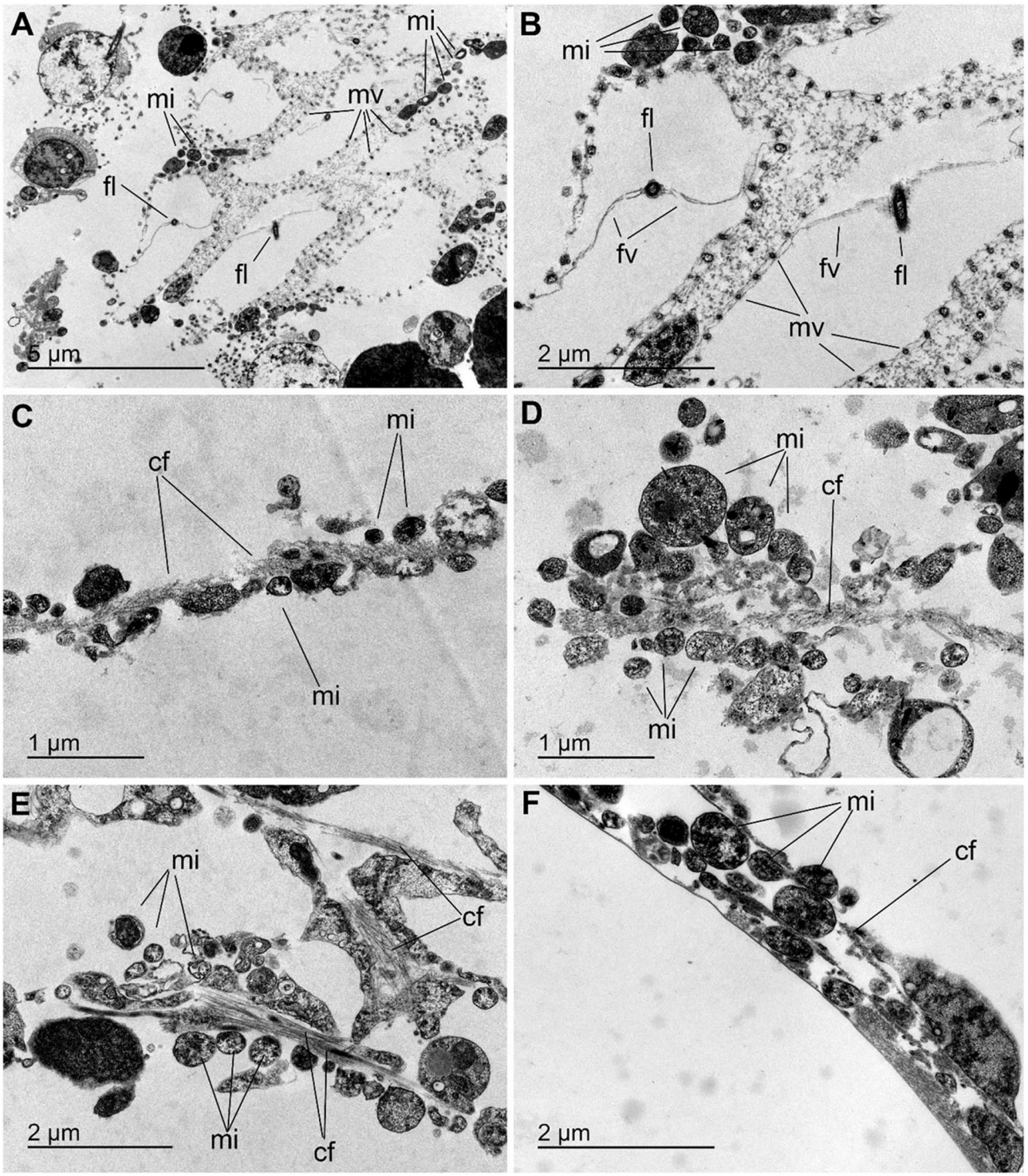


**FIGURE 7 |** Microbes in *Schaudinnia rosea.* **(A,B)** View of flagellated chambers showing the collar bodies with their microvilli (mv) and a flagellum (fl) provided with flagellar vanes (fv). Small groups of prokaryotic microorganisms (mi) occur intracellularly associated to the thin cytoplasmic zones sandwiched between the microvilli of adjacent collar bodies. **(C–F)** Views of small groups of microbes (mi) that gather around the packs of collagen fibrils (cf) that run across the thin mesohyl bands located within the trabecular strands of the sponge body.

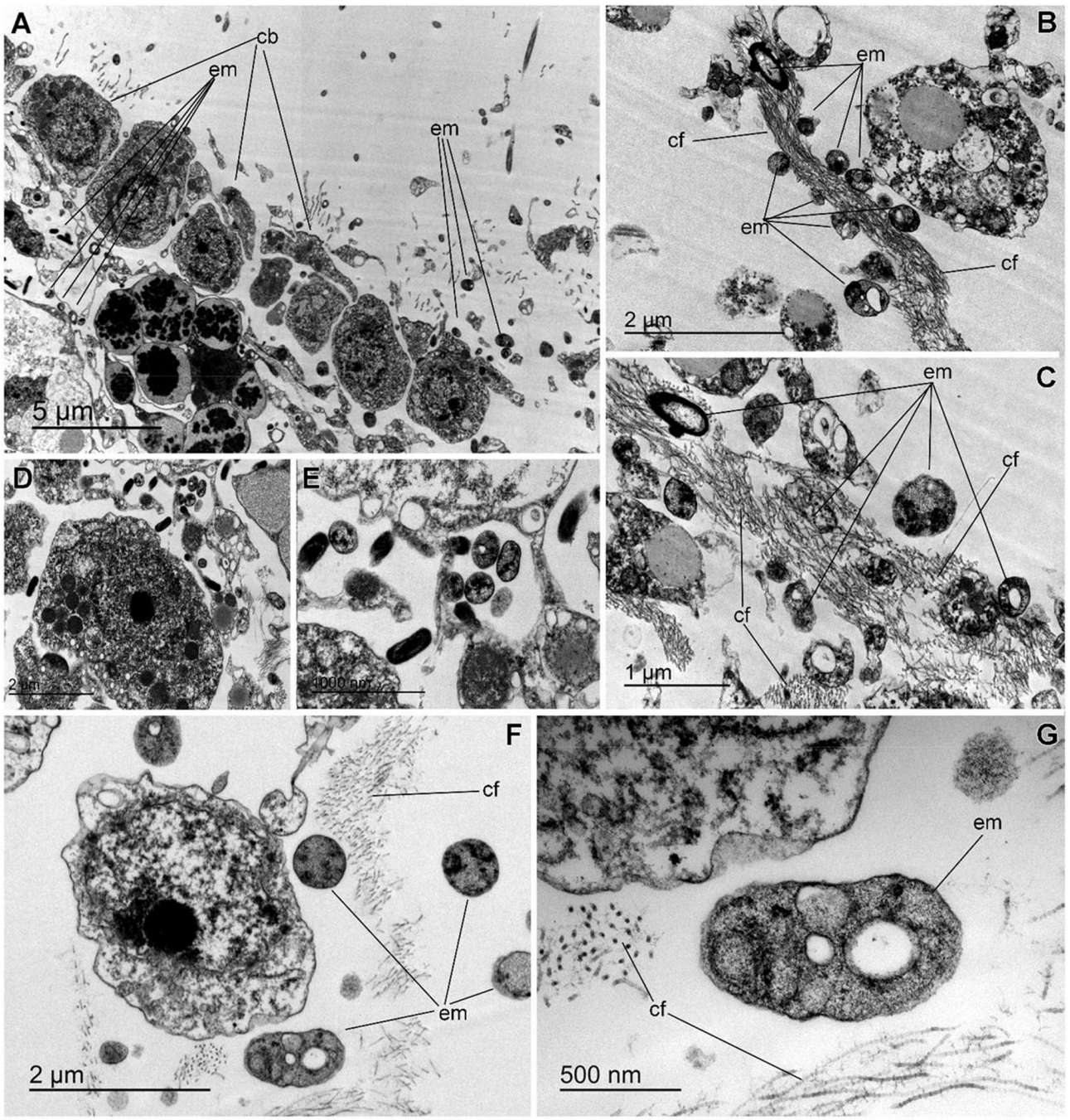


**FIGURE 8 |** Extracellular microbes in *Vazella pourtalesii.* **(A)** Partial view of flagellated chamber, showing the collar bodies (cb) and the underlying trabecular tissue, which is relatively poor in extracellular microbes (em). **(B,C)** Images showing that, in the mesohyl, the extracellular microbes (em) often proliferate in close association to accumulations of collagen fibrils (cf). **(D,E)** Two enlargements of a zone of the trabecular tissue where electron-dense rod-like microbes occur adjacent to coccoid microbes contained intracellularly into a cytoplasmic vesicle of a sponge cell. **(F)** Comparative view of different microbial morphologies, typically characterized by a variety of electron-clear and/or electron-dense granules and cell sizes smaller than 1 µm. **(G)** Detail of an unidentified extracellular microbial cell (em) showing a variety of intracytoplasmic granules. Note the collagen fibrils (cf) around the microbe.

ample aquiferous spaces run. The ultrastructural TEM approach revealed that extracellular microbes of both coccoid and rod-like shape are scattered in both species, but at low density (**Figures 7**, **8**). In *S. rosea*, small groups of microbes were also found intracellularly in the thin cytoplasmic bands that separate the microvilli of adjacent collar bodies (**Figures 7A,B**). However,

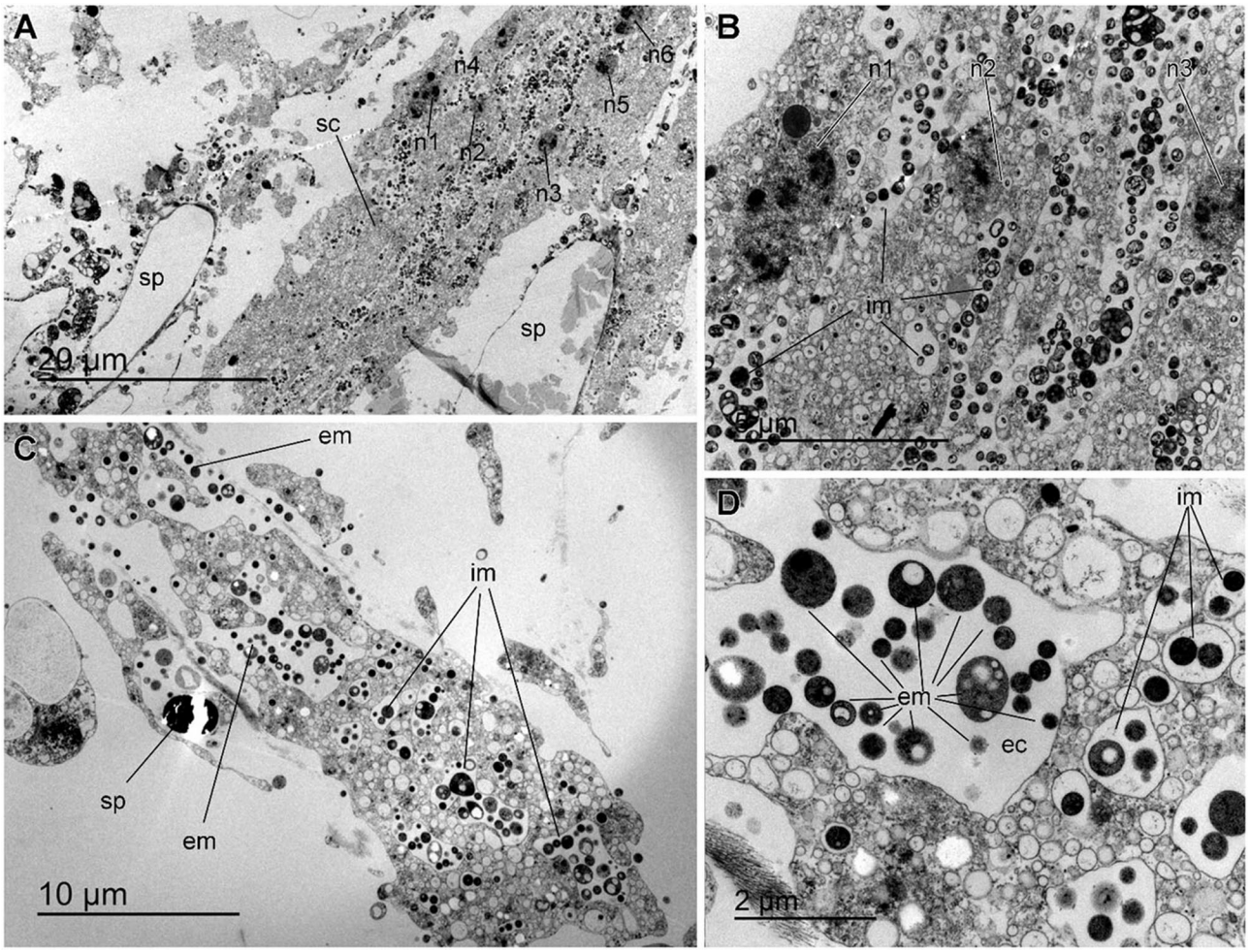


**FIGURE 9 |** Bacteriosyncytia in *Vazella pourtalesii*. **(A)** Partial general view of a bacteriosyncytium (sc) in which six nuclei (n1 to n6) can be seen, along with many intracellular microbes (im). The cell is in a tissue zone where the whole of two large spicules (sp) occurred before we desilicified them for tissue sectioning. **(B)** Enlargement of a zone of the **Figure 8A** in which nuclei n1 to n3 can be seen along with large abundance of intracellular microbes within membrane-bound vesicles. **(C)** Partial general view of bacteriosyncytium, showing abundant intracellular microbes (im), along with abundance of extracellular microbes (em), which proliferate around the syncytium and particularly in the valleys formed by the pseudopodia of the bacteriosyncytium. Because this tissue was not desilicified for sectioning, remains of a silica spicule (sp) can be seen by the side of the bacteriosyncytium. **(D)** Enlargement of **Figure 8C** detailing the variety of sizes and ultrastructure of intracellular microbes (im) within membrane bound vesicles in the cytoplasm of the bacteriosyncytium. Note the presence of extracellular microbes (em) in a large extracellular cavity (ec) formed among the pseudopodia of the bacteriosyncytium.

most of the small groups of microbes occurred extracellularly, associated to the collagen fibrils of the mesohyl matrix in the thin trabecular strands (**Figures 7C–F**, **8**). The relative paucity of extracellular microbes across most of the studied tissue in both sponge species suggested that the extracellular microbial populations are too poor as for being entirely responsible by themselves for the important N fluxes detected in the sponges, particularly in *V. pourtalesii*. In this regard, we discovered large (>70 µm) amoeboid, multinucleate syncytia in *V. pourtalesii*, which are charged with high density of microbes (i.e., archaea and bacteria) in a variety of morphological types. Most of them were coccoid forms smaller than 0.8 microns in their largest diameter (**Figures 9**, **10**). To our knowledge, this is the first description in hexactinellid sponges of a cytological system specialized in holding microbes. These hexactinellid cytological system is herein referred to as bacteriosyncytia, being the cytological analogous of the non-syncytial bacteriocytes known from demosponges (e.g., Maldonado, 2007). It is worth noting that the microbes were not in direct contact with the cytoplasmic environment of the bacteriosyncytia but they were included in a membrane-bound vesicle. Each vesicle contained one or few bacteria from either identical or different morphological types. Most bacteria contained one to several intracytoplasmic granules and compartments. At the present moment, a correspondence between the microbial morphotypes and the genome-defined groups remains uncertain. Importantly, many of the microbes in the vesicles appeared to be partially degraded or digested, suggesting that the sponge

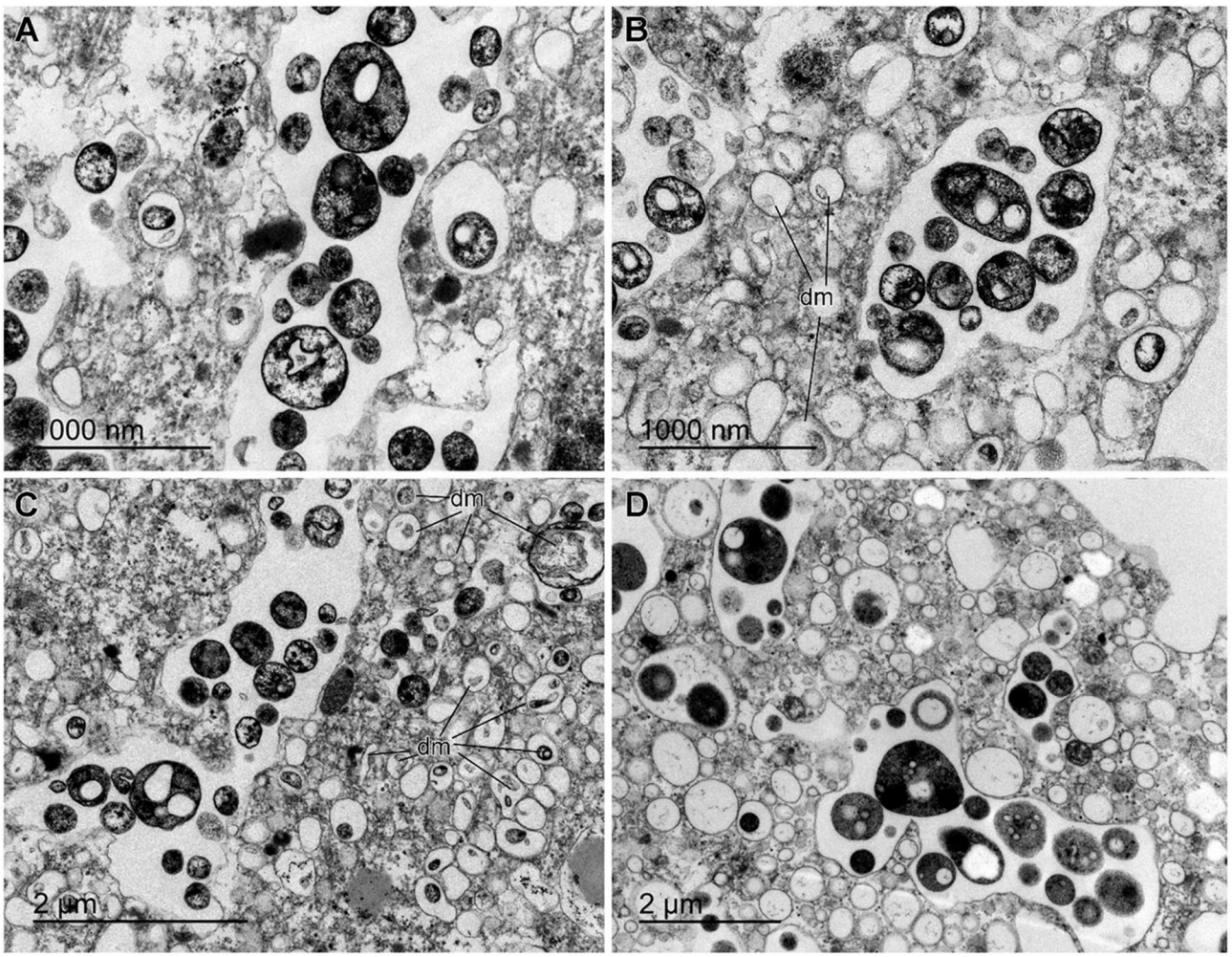


**FIGURE 10 |** Details of bacteria in the bacteriosyncytia of *Vazella pourtalesii*. **(A–D)** Diversity of intracellular microbes hosted in either individualized or collective membrane-bound vesicles. Coccoid cell shapes predominate, typically characterized by one or several granules and inclusions. Documented microbial sizes rarely exceed 0.8 µm in the largest diameter. Some of the microbes appear to be degraded or digested within the vesicles (dm).

is feeding at some point on the microbes farmed into the bacteriosyncytia (see Discussion). It was also documented that the microbes proliferated in abundance extracellularly but only in the close periphery of the bacteriosyncytia (**Figures 9C,D**: em), and particularly in the valleys formed by the large pseudopodia emitted by the bacteriosyncytia. Bacteriosyncytia were not detected in *S. rosea*, but a more extensive body sampling would be required to definitively discard their occurrence.

## Nutrient Utilization Throughout the Hexactinellid Grounds

Annual flux rates for the several studied nutrients through the aggregations of *V. pourtalesii* on the Scotian Shelf were estimated (**Supplementary Data File 2**) from the average flux rates depicted in **Figure 3A**. It was calculated that the sponge grounds consume annually 144.8 ± 334.2 × $10^6$ mole of ammonium, while simultaneously releasing 594.2 ± 232.2 × $10^6$ mole of nitrite, 93.2 ± 66.1 × $10^6$ mol of nitrate, and 20.5 ± 12.8 × $10^6$ mole of phosphate (**Figure 11**).

# DISCUSSION

## Net Flux of Nutrients and Ecological Implications

The analysis of the net flux of nutrients reveals several patterns: (1) the processing of ammonium and nitrite appears to be markedly different between the two investigated hexactinellid species, despite *V. pourtalesii* and *S. rosea* being phylogenetically related as members of the family Rossellidae; (2) both species are consistently small sources of phosphate, a pattern also in agreement with nearly all studies on demosponges; and (3) both species have strong inter-individual differences in the magnitude and sign of the nitrate flux, with some individuals being net sources and others being net sinks.

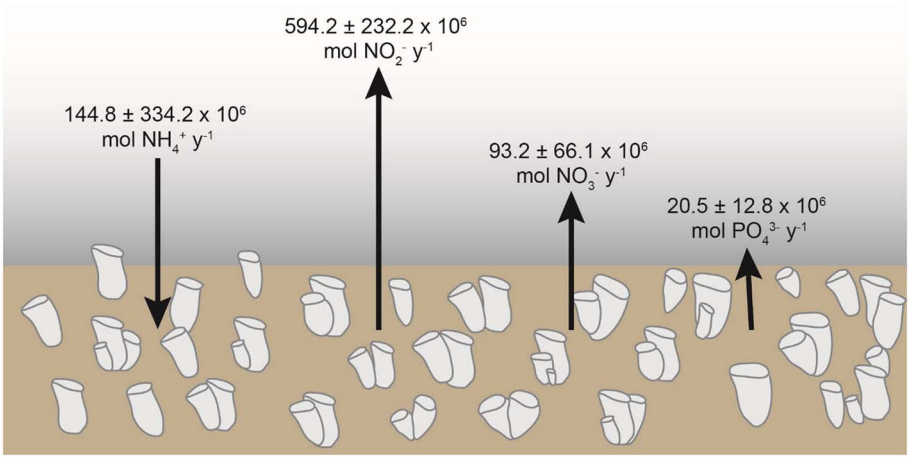


**FIGURE 11 |** Summary of the annual net flux of ammonium ($NH_4^+$), nitrite ($NO_2^-$), nitrate ($NO_3^-$), and phosphate ($PO_4^{3-}$) across the aggregations of *Vazella pourtalesii* at the Scotian Shelf (Canada).

Another interesting feature is that most individuals of *V. pourtalesii* shifted from being net consumers of ammonium to being net releasers after a few days exposed to the laboratory conditions (**Figure 3C**). Those conditions included the use of coastal seawater with similar temperature and ammonium concentration than those in the natural habitat of the sponges but twice nitrite concentration and half of nitrate (**Supplementary Table 2**). This coastal water, close to the big city of Halifax, is also assumed to be characterized by different populations of microbes in suspension and higher quantities of total organic matter than available in the natural offshore habitat. Unfortunately, neither the microbial populations in the laboratory seawater nor in the tissue of the laboratory-maintained sponges were investigated after the experiments. Therefore, because of several uncontrolled factors, the exact reasons of the shift in the ammonium flux remain unclear. One of the most plausible hypotheses is that the original composition of the sponge microbiota associated to the processing of ammonium experienced a progressive detrimental shift after being exposed for to laboratory water. A mechanism for that process would be a much higher level of oxygenation of the seawater (95% in laboratory water versus <43% in the sponge habitat), which may favor the colonization of the sponge tissue by lineages of coastal microbes, which would displace part of the original microbiota. If this is so, it means that the functional integration between the sponge and the microbes involved in the ammonium routes is more delicate and habitat-dependent than that involved in the phosphate metabolism. In line with this view, a recent study revealed significant differences in the microbiota between individuals of *V. pourtalesii* grown on natural substrata and individuals grown on adjacent artificial substrata that raised a mere couple of meters from the sea bottom (Busch et al., 2021). The individuals growing on the artificial substratum were significantly enriched in Bacteroidetes, Verrucomicrobia and Cyanobacteria compared to those growing on natural substrata. In the only two other hexactinellid sponges where nutrient fluxes have been investigated so far, *Aphrocallistes vastus* (Fam. Aphrocallistidae) and *Rhabdocalyptus dawsoni* (Fam. Rossellidae), ammonium was released by both species (Yahel et al., 2007). The flux determination in both species was conducted by the in-ex methods, which yielded instant flux rates of 0.201 ± 0.128 μmol $L^{-1}$ and −0.388 ± 0.068 μmol $L^{-1}$, respectively. Those nutrient instant rates can be neither compared to those measured in our incubations nor scaled up to the entire sponge populations.

When the net flux rate of ammonium consumption by *V. pourtalesii* was scaled up through the extension of the sponge aggregations on the Scotian Shelf, an annual ammonium demand of 144.8 ± 334.2 $\times 10^6$ mole (some 2.6 million kg; **Figure 11**) was estimated. The significance of this figure emerges more clearly when the hourly rate of ammonium consumption by *V. pourtalesii* (5.9 μmol $L^{-1}$ of sponge tissue $h^{-1}$) is compared to the ammonium consumption (47 × $10^{-3}$ μmol $L^{-1}$ of seawater $h^{-1}$) measured for the marine plankton community (bacterioplankton + phytoplankton) of a coastal area in the eutrophic Baltic Sea (Klawonn et al., 2019). The comparison reflects that a *V. pourtalesii* individual of 1 liter in body volume consumes about three orders of magnitude more ammonium than the entire plankton community in a liter of eutrophic coastal seawater, which, in turn, is known to have higher rates than those of the plankton community in worldwide oceanic and estuarine systems (Klawonn et al., 2019). This incorporation of external ammonium by the sponges to fuel the internal microbiota is not ecologically inconsequential, since it may decrease the ammonium availability for the free-living microbial populations in the seawater of the sponge habitat. Indeed, the ammonium concentration at the sponge habitat is abnormally low, ranging from 0.04 to 0.56 μM (**Table 2**). Ammonium being one of the main N nutrient of the bacterioplankton, its depletion through the sponge uptake is assumed to have negative effects on the development of the bacterioplankton community. A poor free-living bacterioplankton community in the demersal water mass around the aggregations of *V. pourtalesii* would decrease the feeding chances for those sponge species that do

not farm their bacteria internally but that rather rely on the filter feeding of external bacterioplankton and picophytoplankton. In line with this view, it has recently being found (Bart et al., 2020) that the bulk energy for the aerobic metabolism of *V. pourtalesii* is not provided by the filter-feeding of the free-living bacterioplankton (only about 10%). Rather, the sponge appears to largely rely on the uptake of dissolved organic matter (about 90%), a carbon source that can be likely processed by both the internal microbiota and the sponge cells (**Figure 6**), as also demonstrated for demosponges (Rix et al., 2020). Therefore, most of the available evidence suggests that the remarkable incorporation of ammonium by *V. pourtalesii* may result in a nutritional competitive exclusion of other sponge species and this may be one of the reasons why the aggregations of *V. pourtalesii* are markedly monospecific. This view is also supported by indirect evidence on other hexactinellid species. For instance, *Schaudinnia rosea,* characterized by low microbial abundance, and *Aphrocallistes vastus*, which apparently lacks an associated microbiota, both release ammonium and both form multispecies sponge assemblages rather than monospecific aggregations. It has already been corroborated that *A. vastus* heavily relies on filter-feeding of external bacteria and other picoplankton, with negligible energetic contribution by incorporation of dissolved organic matter (Yahel et al., 2007; Kahn et al., 2018). Certain groups of filter-feeding organisms, such as bivalves, are known to have large filtration ability (up to 100 $m^3$ $m^{-2}$ $d^{-1}$) for phytoplankton, an activity that has been shown to regulate directly primary production in the local systems where bivalves thrive (Kimmerer et al., 1994). The energy requirements estimated for several species of shallow-water sponges have revealed that some of them must process particles at the same order of magnitude as some bivalves (reviewed in Gili and Coma, 1998). The ecological effects of such sponge activity have seldom been quantified in terms of food limitation, but there is indirect evidence of their ecological relevance. For instance, picoplankton is frequently depleted in the water layer overlying coral reefs and the filter-feeding activity of sponges has been suggested to be one of the main drivers (de Goeij and Van Duyl, 2007; Nelson et al., 2011). In summary, despite growing suspicion that competition by particulate food may be a relevant factor in the sponge aggregations, the process has not yet being properly quantified in any aggregation and its role remains poorly understood (Maldonado et al., 2017).

Regarding nitrite, the notable release rate by *V. pourtalesii* (i.e., 24.3 μmol per liter of sponge tissue and hour, and some 27.3 million kg at the sponge ground level annually) is also thought to be of some ecological significance. The nitrite is an intermediate product used as a source of nitrogen by the phytoplankton and, in a more important way, by the bacterioplankton. Because in seawater the nitrite concentration is typically low, the important nitrite release by the sponges is expected to favor the co-existence of different populations of nitrifiers, avoiding the typical competitive exclusions driven by low nitrite + low ammonium availability (Zakem et al., 2018). A majority of HMA demosponges consume ammonium and release nitrite (Scheffers et al., 2004; Jiménez and Ribes, 2007; Morganti et al., 2017), just as *V. pourtalesii* does. From this perspective, and given that the bacteriosyncytia contain large amounts of microorganisms, *V. pourtalesii* would be functionally closer to HMA demosponges and *S. rosea* to LMA demosponges, but without actually fitting in such categories. Although bacteriosyncytia have not been detected in our TEM exploration of *S. rosea*, additional studies involving sampling of more individuals and more body regions would be required to discard their occurrence definitively.

The nitrate released by the *V. pourtalesii* ground ($93.2 \times 10^6$ mol or some 5.8 million kg) is of far lower magnitude than the nitrite release, with most of its further consumption being expected to be due to the phytoplankton community once the nitrate rich demersal water of the sponge ground is uplifted to the photic zone by any of the advective processes contributing to water mixing on continental shelves.

The phosphate release in the two hexactinellid species herein investigated agrees with the only other measurement available for Hexactinellida, which reported in *Aphrocallistes vastus* a low release of phosphate at instantaneous rates of $35 \pm 80 \times 10^{-3}$ μmol $L^{-1}$ (Yahel et al., 2007). Low rates of phosphate release have also been detected in most investigated demosponges (Maldonado et al., 2012; Ribes et al., 2012; López-Acosta et al., 2019). Through the entire sponge ground of *V. pourtalesii*, we have estimated an annual release of $20.5 \times 10^6$ mol of phosphate, which represent some 1.9 million kg of phosphate. Because phosphate is known to be a limiting nutrient in many bacterioplankton and phytoplankton communities (Smith, 1984; Brembu et al., 2017), the low but continuous release of phosphate by sponges is expected to have positive effects on the development of microplankton communities at the regional scale.

In our study, we found no significant relationship between nutrient flux rate and ambient concentration for any nutrient in any of the two species (**Supplementary Figure 1**). One of the reasons is that, at the time of our sampling, the between-site variation in the ambient concentration of the investigated nutrients in the bottom seawater of the sponge grounds was minimal (**Tables 1**, **2**). However, changes in concentration may occur between summer and winter conditions (Petrie et al., 1999; Maldonado et al., 2021). Future studies would be advisable to evaluate how episodic and/or seasonal changes in the biogeochemistry of the sponge habitat may affect the net nutrient fluxes of the sponges and the composition of their microbiome. Investigations of nutrient flux rates in different populations and/or subpopulations of the HMA, Caribbean demosponges *Xetospongia muta* and *Ircinia felix* revealed between-site differences in the ambient concentration of inorganic nutrients and also in the magnitude and sign of the flux rate for some of those nutrients (Fiore et al., 2013; Archer et al., 2017). Despite the absence of information on the plausible between-site differences in the microbiome of those sponges, the studies concluded that functioning as sink or source was mostly a direct response of the sponges to the differences in the ambient concentration of the nutrients. Nevertheless, our findings on the metabolic intricacies of the sponge microbiome suggest that the underlying mechanism behind the sponge holobionts shifting from being sources to sinks or vice versa for a N nutrient must involve more complex

processes than a mere modest change in the ambient nutrient concentration. The idea that nutrient flux rates in HMA sponges can somehow be predicted from ambient nutrient concentrations neglects the metabolic and physiological complexity behind such flux rates: there will always be biological confounding factors seriously interfering the mathematical relationship between the two parameters of the regression. For instance, in the case of the ammonium flux rate in *V. pourtalesii*, the important incorporation of external ammonium by the sponges suggested, *a priori*, a negative correlation between consumption rate and ambient concentration, but no significant correlation was detected (**Supplementary Figure 1**). The reason may be that the ammonia excretion of the sponge cells supplies ammonium internally, obscuring the expected mathematical relationship between the ambient concentration of ammonium and the rate of ammonium incorporation by the sponges. Yet, in this particular example, more interferences overlap, because ammonium is also internally generated by dissimilatory nitrate reduction and by the "denitrification+fixation" pathways. Therefore, the intertwining of processes generating ammonium internally advises against the idea of interpreting the rate of ammonium incorporation as a mere function of its ambient concentration, since it is not straightforward relationship and may lead to report spurious (i.e., biologically meaningless) correlations. This situation may applies to all other inorganic nutrients with high microbial involvement.

Another uncertainty relative to the determination of sponge flux rates is the methodological approach: sampling the inhalant and exhalant water flows of the sponges (in-ex method) versus incubating the sponges for a given period of time. Both methods have pros and cons. Although it is always difficult to predict how the confinement of a sponge in an incubation chamber may affect its physiology, we have indirect evidence that the assayed sponges remained healthy and physiologically active through the 24 h incubations. We sequenced the transcriptome of six individuals of *V. pourtalesii* subjected to successive laboratory incubations for 24 h in 16L of seawater to examine their silicon consumption. The analysis of differential gene expression revealed no sign of anoxia, stress, starvation or apoptosis in the incubated sponges, compared to wild control sponges (Maldonado et al., 2020). Rather, the sponges were actively incorporating silicon for skeletal and body growth. Additionally, there was not a single casualty during either the *in-situ* incubations or the 2 weeks of laboratory experiments.

## Integrating the Nitrogen Pathways of the Microbiome

Nitrification is a key process in oceanic N cycling as it oxidizes ammonia *via* nitrite to nitrate, which is the main source of nitrogen for many marine primary producers. There are two functionally distinct groups of aerobic microbes involved in the nitrification process: (1) bacteria and archaea that oxidize ammonia to nitrite (i.e., ammonia-oxidizing bacteria and archaea, previously referred to as AOB and AOA); (2) bacteria that oxidize the resulting nitrite to nitrate (i.e., nitrite-oxidizing bacteria, referred to as NOB) and that are often named with the prefix "Nitro," such as *Nitrospinae*, *Nitrospirae*, *Nitrococcus*, etc. To date, no organism is known to carry out both oxidation steps.

Oxidation of ammonia/ammonium to nitrite has been studied quite intensively in marine shallow-water demosponges (Diaz and Ward, 1997; Jiménez and Ribes, 2007; Bayer et al., 2008; Southwell et al., 2008a; Hoffmann et al., 2009; Schläppy et al., 2010; Ribes et al., 2012; Morganti et al., 2017; Subina et al., 2018), with the abundance of AOA being more important than that of AOB both in marine sponges (Radax et al., 2012; Steinert et al., 2020) and, in general, also in the seawater (Francis et al., 2005; Wuchter et al., 2006). In this regard, Van Duyl et al. (2008) reported nitrite release by individuals of *Nodastrella nodastrella*, another rossellid hexactinellid. Those results are in full agreement with our findings on *V. pourtalesii*, a sponge releasing important amounts of nitrite, because its further oxidation is not possible or it happens at very low rates. However, this was not the case of *S. rosea*, which showed nitrite flux rates to be around zero. These two different physiological responses involve that nitrite oxidizing bacteria (NOB) are absent in the tissue of *V. pourtalesii* but not in that of *S. rosea*. The metagenome analysis corroborated such an interpretation, since genes responsible for nitrite oxidation to nitrate were not found in *V. pourtalesii*, neither in MAGs nor in the unbinned metagenomic contigs.

The nitrite oxidizing bacteria, although less investigated in sponges than the ammonium oxidizing microbes, have also been found recurrently as part of the microbiota of demosponges (Thomas et al., 2016; Moitinho-Silva et al., 2017). Their functional role has been made evident through both a consistent excretion of nitrate by the sponges (Jiménez and Ribes, 2007; Bayer et al., 2008; Ribes et al., 2012; Leys et al., 2017; Subina et al., 2018) and metagenomic studies (Bayer et al., 2014). The absence of these genes in the microbiota of *V. pourtalesii* and probably in that of *N. nodastrella* (Van Duyl et al., 2008) opens new questions about its significance for the sponge physiology and ecology. The fact that most individuals of *V. pourtalesii* shifted their initial condition of ammonium consumers toward net ammonium releasers after being exposed to laboratory conditions different from those in the sponge habitat strongly suggests that the sponge microbiota involved in the nitrification is markedly habitat-dependent in at least this sponge species. The noticed shift in the nitrification likely derived from the AOA and AOB populations being negatively affected or even largely replaced by new microbial populations favored by the conditions of the coastal seawater that fed the laboratory.

The negative relationship between ammonium consumption and nitrite release by *V. pourtalesii* (**Figure 4A**) suggests that most released nitrite derives from a first step in nitrification, which cannot be processed further in the sponge through nitrification (**Figure 6**). Yet, we suggest that part of the nitrite produced by the nitrification is not released but rather diverted toward the aerobic process of denitrification and the anaerobic DNRA pathway, so that those three major pathways become bridged through their intermediate steps (**Figure 6**: bridge B1) rather than through the more conventional production of nitrate by nitrification (**Supplementary Table 4**). While the DNRA pathway yields as final product ammonium to close a N cycle in the holobiont (**Figure 6**), denitrification yields as final product inert nitrogen gas ($N_2$) that needs to enter the N-fixation pathway to become ammonium through the nitrogenase of Mycoplasmatales and Plantomycetota (**Figure 6**).

Nitrogen fixation has also been reported in shallow-water sponges (Wilkinson and Fay, 1979; Wilkinson et al., 1999; Mohamed et al., 2008; Ribes et al., 2015), reducing biologically inaccessible $N_2$ gas to ammonium and representing a source of dissolved inorganic nitrogen (DIN) additional to that available by sponge feeding.

The coupling/bridging among these four pathways to close a N cycle in *V. pourtalesii* (**Figure 6**) is not trivial, as the aerobic metabolism of the holobiont becomes connected to anaerobic and facultative chains of reactions, what helps to explain how these sponges are able to deal with the low oxygen conditions (<60%) that often characterize deep-sea benthic habitats. The oxygen concentration in the bottom water of the *V. pourtalesii* grounds is only 2.8 ml $L^{-1}$ (Beazley et al., 2018), a mere 42.4% relative to the maximum oxygen values occurring in the superficial waters of that area. In the absence of NOB within the sponges, the main source of nitrate to fuel the denitrification pathway remains intriguing (**Figure 6**), as some individuals of *V. pourtalesii* consumed nitrate from seawater while others released it (**Figure 4B**, **Table 2**). The nitrate concentration in the deep-water habitat of *V. pourtalesii* is relatively high (17.2 μM) compared to that in the coastal water (7.9 μM) and could well cover the sponge's demands. From our current approach, it also remains unclear whether a full microbial denitrification from nitrate to $N_2$ gas can be accomplished in *V. pourtalesii*. On the one side, the genes coding for nitrate and nitrite reductases have been identified reliably. On the other side, the occurrence of the genes coding for the enzymes involved in the last two denitrification reactions (nitric oxide reductase and nitrous oxide reductase) was not as certain (**Figure 6**). The nitrous oxide reductase was not found in MAGs, but it was detected in the unbinned data, making it impossible to assign a microbial lineage for this activity. More importantly, the nitric oxide reductase, which converts nitric oxide (NO) into nitrous oxide ($N_2O$) was detected in neither the MAGs nor the unbinned data. This would mean that the produced nitric oxide —a highly toxic intermediate compound with a lifetime of just seconds but able to diffuse freely across membranes with relevant roles as signaling molecule (Hancock, 2017)— could not be further processed to complete denitrification. Yet, we suggest that denitrification can be completed in *V. pourtalesii* because nitrous oxide is available as an intermediate product from the DNRA pathway (**Figure 6**: bridge B2). Because our findings leave some unanswered questions and unresolved aspects regarding denitrification, disentangling the metabolic integration of the denitrifying microbes in *V. pourtalesii* will require further research. Some sponge grounds consisting essentially of an assemblage of deep-water astrophorid demosponges have shown high denitrification activity (i.e., similar in rate values to those of marine sediments). Denitrification in those astrophorid grounds was so intense that the sponges were estimated to incorporate a large part of the nitrate available in the seawater of their habitat (Rooks et al., 2020). From the available results in *V. pourtalesii*, the conventional coupling of nitrification to denitrification through nitrate does not appear to happen (**Figure 6**): the nitrifying enzymes for the conversion of nitrite into nitrate are missing. Likewise, the coupling of denitrification to nitrification through the process of $N_2$ fixation is not happening through the common pathways, since the enzymes responsible for converting nitric oxide (NO) into nitrous oxide ($N_2O$) are not yet found in this sponge species (**Figure 6**), but nitrous oxide diverted from the DNRA pathway allows to produce the final $N_2$ product of denitrification that feeds the nitrogen fixation. Therefore, two bridges among major nitrogen pathways —which would be mediated through intermediate N by-products— are required for the microbiome to close efficiently the N cycle in the sponge.

We have found little evidence of anaerobic ammonium oxidation (anammox), in which ammonium and nitrite are converted into $N_2$ and water. In contrast, some studies on demosponges have found nitrification to be coupled with denitrification and anammox (Hoffmann et al., 2009; Schläppy et al., 2010; Fiore et al., 2013). Genes involved in the production of urea or its hydrolysis have not been found either.

By combining the functional roles of the detected N-involved enzymes in the microbiome of *V. pourtalesii* (**Supplementary Table 4**), most of the nutrient fluxes that we measured in the living sponges (**Figure 3**, **Table 2**) become explained by the microbial metabolic pathways (**Figure 6**). Nitrite and nitrate are often products of nitrification processes and, if not used in other microbial processes, excreted. In some demosponges, nitrite release was not detected (as it is also the case of *S. rosea*) and only the final product, nitrate, was released (Bayer et al., 2008). In the present study, nitrite excretion in *V. pourtalesii* may be explained by a higher abundance of ammonia-oxidizing microbes (Radax et al., 2012; Steinert et al., 2020) and the absence or low abundance of nitrite-oxidizing bacteria (NOB) and microbes relying on nitrogen reduction pathways (denitrification, nitrate and/ or nitrite reduction). Indeed, genes responsible for nitrite oxidation, which are typical of NOB, were neither found in MAGs nor in the unbinned metagenomic data. NOBs appear to have a high mortality rate (Kitzinger et al., 2020), probably resulting in underestimation of their abundance, which might be the reason why we could not detect the functional genes in the metagenome data. Variable nitrate fluxes (excretion and/or uptake), depending on the individuals, might be a result of unbalanced nitrification-nitrate reduction (DNRA, denitrification) coupling due to transient changes in physiological rhythms (e.g., pumping activity) that may change oxygen availability and the effectiveness sensitivity of some of the involved enzymes.

A large proportion of microbes in *V. pourtalesii* appear able to assimilate ammonia/ammonium (**Figure 6**), which could explain the incorporation of ammonium from seawater detected during the sponge incubations. Collectively, the identified pathways of the microbial N metabolism support the notion that the ammonium incorporated from seawater, along with the ammonia excreted by the sponge cells (which undergoes molecular auto-ionization to form ammonium and amide ions), and along with the ammonia/ammonium resulting from the DNRA and the denitrification+N fixation pathways, supply the microbiota of *V. pourtalesii* with this crucial substratum that, through N assimilation, fuels its growth (**Figure 6**). The detection of prokaryotic glutamine synthetase and glutamate dehydrogenase in the MAGs (**Supplementary Table 4A**) suggests

that a large part of the microbiota N assimilation occurs through ammonification of ammonia to produce basic amino acids, as already concluded for the SAR3254 symbiont in a previous study of *V. pourtalesii* (Bayer et al., 2020). The recent finding that *V. pourtalesii* covers its energetic demands mostly (90%) through uptake of dissolved organic carbon (DOC) rather than through filter feeding (10%) of bacterioplankton and other particulate carbon (Bart et al., 2020) also suggests that a substantial part of the DOC taken up by the sponges could indeed not be used by the sponge cells themselves but running through the assimilation pathway of the microbiota (**Figure 6**), as it has also been shown for some HMA demosponges (Rix et al., 2020).

The finding that most of the sponge-associated microbes in *V. pourtalesii* appear to live within large, amoeboid syncytia (**Figures 7–10**) has also important functional implications: (1) the proliferation of microbes may be under a better control by the sponges; (2) the microbes can be potentially transported readily toward the required tissue areas for dealing with waste and/or to ensure the optimal redox conditions for the needed metabolic routes; (3) the microbes, farmed by the sponge out of both its waste and the incorporation of ammonium and DOC, can be readily digested within the syncytia, potentially becoming an internal food source that is independent from the availability of external particulate food (**Figure 6**). Therefore, the complex N microbial engine that internally provides food to the sponges may constitute an important adaptive advantage for these sponges to cope with starvation during periods of limited food supply to the deep-sea habitat. Collectively, our physiological, ultrastructural, and genetic findings support the idea of a N biochemical network entailing not only the various microbial lineages but also the cell metabolism of the sponge, so that the correct metabolic functioning of the *V. pourtalesii* holobiont will depend substantially on the correct functioning of its N microbial engine.

## Phosphate Release

Phosphate (or orthophosphate ion, $PO_4^{-3}$) is the most bioavailable form of phosphorus in the biosphere. Its availability has long been identified as a key determinant of marine productivity and its cycling is closely linked to carbon and nitrogen dynamics in the oceans (Villarreal-Chiu et al., 2012). Dissolved organic phosphorus (DOP) accounts for up to 80% of total soluble P and is rapidly utilized by the microbial fraction in oligotrophic waters (Björkman and Karl, 2003), playing a pivotal role in driving growth, community composition and population dynamics of free-living marine microorganisms (Dyhrma et al., 2007). Phosphonates are widespread in nature in a range of biogenic molecules, representing an important component of marine DOP. Unlike the more common C–O–P bond characterizing most biological compounds containing phosphate, phosphonates are characterized by a highly stable —and apparently ancient— direct carbon–phosphorus (C–P) bond (Ternan et al., 1998; White and Metcalf, 2007), which resists biochemical, thermal, and photochemical decomposition. Phosphonates are produced by many primitive life forms, including a wide range of marine invertebrates in which the phosphate bound in phosphonates may comprise as much as 50% of the total P content (Quin, 2000). Such natural-product phosphonates are 2-aminoethylphosphonic acid (2-AEP; ciliatine) or 2-amino-3-phosphonopropionic acid (phosphonoalanine), which are found as side groups on exopolysaccharides or glycoproteins, or in the polar head groups of membrane phosphonolipids. There are quite some enzymes found to be responsible for degradation/utilization of such substances (for reviews see Ternan et al., 1998; Villarreal-Chiu et al., 2012).

Our results suggest that at least some microorganisms in the *V. pourtalesii* microbiome are able to utilize host-derived organo-phosphonates, such as representatives of Planctomycetota, Crenarcheota, Gamma- and Alphaproteobacteria. We did not look for biosynthesis pathways of phosphonates. Even if phosphate is either re-used by sponge-associated microbes or the host itself, the final outcome is a low rate of phosphate release from the sponges, as it was measured in the incubations of *V. pourtalesii* and *S. rosea* (**Figure 3**, **Tables 1**, **2**). However, there are many remaining gaps in the current understanding of the utilization of P by sponge-associated microbes, as well as on their functional integration in the sponge metabolism.

# CONCLUSIONS

Our study reveals that important physiological differences occur between the hexactinellid sponges *Schaudinnia rosea* and *Vazella pourtalesii*, despite them being phylogenetically closely related as members of the family Rossellidae. Differences were particularly important regarding the net flux of ammonium and nitrite. The MAG study of the *V. pourtalesii* microbiome revealed a rich community of archaea and bacteria driving nitrification, denitrification, DNRA, nitrogen fixation, and ammonia assimilation. The various biochemical microbial pathways are partially coupled and/or bridged to each other closing a N cycle in the sponge and internally generating ammonium, which, through assimilation, appears to sustain the bulk of the sponge microbiome. The ammonium needs of the sponges to fuel their internal microbiota are so large that they cannot be fulfilled by the internal N cycle and ammonium has to be incorporated from seawater. It is here estimated that about 2.6 million kg of ammonium are taken up annually from the bottom water by the aggregations of *V. pourtalesii* established at the deep zone of the Nova Scotia continental shelf. It is herein postulated that such an important ammonium removal has a negative impact on the development of the free-living bacterioplankton around the sponge aggregations. An impoverished bacterioplankton community may reduce the feeding chances of the many sponge species that rely on filter feeding free-living bacteria. Such a nutritional competitive exclusion would explain, along with other factors, why the aggregations of *V. pourtalesii* are markedly monospecific. This sponge species appears to nourish out of the digestion of its microbiota, which is mostly farmed within its bacteriosyncytia through a network of nitrogen-based biochemical reactions revolving around the processing of ammonia/ammonium. Beside the ammonium intake, the sponges also affect the deep-sea

ecosystem through an important annual release of nitrite (some 27.3 million kg) and, in smaller quantities, of nitrate and phosphate. The finely tuned metabolic integration among various N-depending microbial lineages and between these and the sponge *V. pourtalesii* suggest that the metabolism of the holobiont depends substantially on the correct functioning of its microbial engine. However, the sponge-microbe functional equilibrium appears to be delicate and can easily be altered just by moving the sponges out of their natural habitat for a few days. Such a susceptibility raises concerns about the need of preserving the habitat conditions in these deep-sea systems. This study also brings in the novel perspective that hexactinellid sponges are not always the slow-metabolism organisms we have traditionally assumed. Some species that grow in dense aggregations may carry intense nutrient exchanges with the surrounding deep-sea environment through a complex metabolic integration with their microbiota and the resulting intense physiological activity has implications of ecological scale for the deep-sea communities.

## DATA AVAILABILITY STATEMENT

The original contributions presented in the study are included in the article and **Supplementary Material**. Detailed sample metadata were deposited in the PANGAEA database: https://doi.pangaea.de/10.1594/PANGAEA.917599, following Bayer et al. (2020). Amplicon and metagenomic raw data including reads and assembled MAGs were deposited in the NCBI database under BioProject PRJNA613976. Individual accession numbers for assembled MAGs are listed in **Supplementary Table 2** of Bayer et al. (2020). Interpro annotation output is available on figshare under https://doi.org/10.6084/m9.figshare.12280313. Further inquiries can be directed to the corresponding authors.

## AUTHOR CONTRIBUTIONS

This study was initially conceived by MM. The first draft was assembled by MM, ML-A, KBa, and KBu, being further refined through input from all co-authors. EK, LB, and HR provided logistic field support for field and laboratory work. EK, LB, MM, and ML-A were responsible for mapping and sponge biomass determination in the *Vazella* grounds. MM and ML-A conducted field and laboratory sponge incubations and scaled up net fluxes. UH, KBa, KBu, and BS were responsible for the amplicon sequencing of the microbiomes of *S. rosea* and *V. pourtalesii*, for sequencing and annotating the metagenome, and metagenome-assembled genomes (MAGs) of the *Vazella* microbial community. MM conducted the histological and TEM study. All authors contributed to the manuscript elaboration at different steps and approved the submitted version.

## FUNDING

This research was funded mostly by the SponGES H2020 grant (BG-01-2015.2, agreement number 679849-2) awarded to HR (coordinator) and the associated international partner consortium. Much of the logistics was also funded by the Fisheries and Oceans Canada International Governance Strategy (IGS) projects awarded to EK and HR. Manuscript elaboration benefited from funding by the Dark-Si grant (MICIU-PID2019-108627RB-I00) to MM.

## ACKNOWLEDGMENTS

The authors thank C. Sitjà and M. García for help with the embedding and sectioning of light microscopy samples. This study is in memory of HR, our co-author, friend, and main coordinator of the H2020 SponGES project, who made this research possible and passed away on 7 March 2020.

## SUPPLEMENTARY MATERIAL

The Supplementary Material for this article can be found online at: https://www.frontiersin.org/articles/10.3389/fmars.2021.638505/full#supplementary-material

## REFERENCES

Archer, S. K., Stevens, J. L., Rossi, R. E., Matterson, K. O., and Layman, C. A. (2017). Abiotic conditions drive significant variability in nutrient processing by a common Caribbean sponge, *Ircinia felix*. *Limnol. Oceanogr.* 62, 1783–1793. doi: 10.1002/lno.10533

Bart, M. C., Mueller, B., Rombouts, T., van de Ven, C., Tompkins, G. J., Osinga, R., et al. (2020). Dissolved organic carbon (DOC) is essential to balance the metabolic demands of four dominant North-Atlantic deep-sea sponges. *Limnol. Oceanogr.* 11652. doi: 10.1002/lno.11652

Bayer, K., Busch, K., Kenchington, E., Beazley, L., Franzenburg, S., Michels, J., et al. (2020). Microbial strategies for survival in the glass sponge *Vazella pourtalesii*. *mSystems* 5, e00473–e00420. doi: 10.1128/mSystems.00473-20

Bayer, K., Moitinho-Silva, L., Brümmer, F., Cannistraci, C. V., Ravasi, T., and Hentschel, U. (2014). GeoChip-based insights into the microbial functional gene repertoire of marine sponges (high microbial abundance, low microbial abundance) and seawater. *FEMS Microbiol. Ecol.* 90, 832–843. doi: 10.1111/1574-6941.12441

Bayer, K., Schmitt, S., and Hentschel, U. (2008). Physiology, phylogeny and *in situ* evidence for bacterial and archaeal nitrifiers in the marine sponge *Aplysina aerophoba*. *Environ. Microbiol.* 10, 2942–2955. doi: 10.1111/j.1462-2920.2008.01582.x

Beazley, L., Wang, Z., Kenchington, E., Yashayaev, I., Rapp, H. T., Xavier, J. R., et al. (2018). Predicted distribution of the glass sponge *Vazella pourtalesi* on the Scotian Shelf and its persistence in the face of climatic variability. *PLoS ONE* 13:e0205505. doi: 10.1371/journal.pone.0205505

Beazley, L. I., Kenchington, E. L., Murillo, F. J., and Sacau, M., del M. (2013). Deep-sea sponge grounds enhance diversity and abundance of epibenthic megafauna in the Northwest Atlantic. *ICES J. Mar. Sci. J. du Cons.* 70, 1471–1490. doi: 10.1093/icesjms/fst124

Björkman, K. M., and Karl, D. M. (2003). Bioavailability of dissolved organic phosphorus in the euphotic zone at Station ALOHA, North Pacific Subtropical Gyre. *Limnol. Oceanogr.* 48, 1049–1057. doi: 10.4319/lo.2003.48.3.1049

Bokulich, N. A., Kaehler, B. D., Rideout, J. R., Dillon, M., Bolyen, E., Knight, R., et al. (2018). Optimizing taxonomic classification of marker-gene amplicon sequences with QIIME 2's q2-feature-classifier plugin. *Microbiome* 6:90. doi: 10.1186/s40168-018-0470-z

Bolyen, E., Rideout, J. R., Dillon, M. R., Bokulich, N. A., Abnet, C. C., Al-Ghalith, G. A., et al. (2019). Reproducible, interactive, scalable and extensible microbiome data science using QIIME 2. *Nat. Biotechnol.* 37, 852–857. doi: 10.1038/s41587-019-0209-9

Brembu, T., Mühlroth, A., Alipanah, L., and Bones, A. M. (2017). The effects of phosphorus limitation on carbon metabolism in diatoms. *Philos. Trans. R. Soc. B Biol. Sci.* 372:20160406. doi: 10.1098/rstb.2016.0406

Busch, K., Beazley, L., Kenchington, E., Whoriskey, F., Slaby, B. M., and Hentschel, U. (2021). Microbial diversity of the glass sponge *Vazella pourtalesii* in response to anthropogenic activities. *Conserv. Genet.* 21, 1001–1010. doi: 10.1007/s10592-020-01305-2

Busch, K., Hanz, U., Mienis, F., Mueller, B., Franke, A., Martyn Roberts, E., et al. (2020). On giant shoulders: How a seamount affects the microbial community composition of seawater and sponges. *Biogeosciences* 17, 3471–3486. doi: 10.5194/bg-17-3471-2020

Callahan, B. J., McMurdie, P. J., Rosen, M. J., Han, A. W., Johnson, A. J. A., and Holmes, S. P. (2016). DADA2: High-resolution sample inference from Illumina amplicon data. *Nat. Methods* 13, 581–583. doi: 10.1038/nmeth.3869

Caranto, J. D., and Lancaster, K. M. (2017). Nitric oxide is an obligate bacterial nitrification intermediate produced by hydroxylamine oxidoreductase. *Proc. Natl. Acad. Sci. U. S. A.* 114, 8217–8222. doi: 10.1073/pnas.1704504114

Chaumeil, P.-A., Mussig, A. J., Hugenholtz, P., and Parks, D. H. (2019). GTDB-Tk: a toolkit to classify genomes with the Genome Taxonomy Database. *Bioinformatics* 36, 1925–1927. doi: 10.1093/bioinformatics/btz848

Chu, J. W. F., Maldonado, M., Yahel, G., and Leys, S. P. (2011). Glass sponge reefs as a silicon sink. *Mar. Ecol. Prog. Ser.* 441, 1–14. doi: 10.3354/meps09381

Cook, S. E., Conway, K. W., and Burd, B. (2008). Status of the glass sponge reefs in the Georgia Basin. *Mar. Environ. Res.* 66(Suppl.), S80–S86. doi: 10.1016/j.marenvres.2008.09.002

Corredor, J. E., Wilkinson, C. R., Vicente, V. P., Morell, J. M., and Otero, E. (1988). Nitrate release by Caribbeaan reef sponges. *Limnol. Oceanogr.* 33, 114–120. doi: 10.4319/lo.1988.33.1.0114

de Goeij, J. M., and Van Duyl, F. C. (2007). Coral cavities are sinks of dissolved organic carbon (DOC). *Limnol. Oceanogr.* 52, 2608–2617. doi: 10.4319/lo.2007.52.6.2608

Diaz, M., and Ward, B. (1997). Sponge-mediated nitrification in tropical benthic communities. *Mar. Ecol. Prog. Ser.* 156, 97–107. doi: 10.3354/meps156097

Dunham, A., Archer, S. K., Davies, S. C., Burke, L. A., Mossman, J., Pegg, J. R., et al. (2018). Assessing condition and ecological role of deep-water biogenic habitats: glass sponge reefs in the Salish Sea. *Mar. Environ. Res.* 141, 88–99. doi: 10.1016/j.marenvres.2018.08.002

Dyhrma, S. T., Ammerman, J. W., and Van Mooy, B. A. S. (2007). Microbes and the marine phosphorus cycle. *Oceanography* 20, 110–116. doi: 10.5670/oceanog.2007.54

Fiore, C. L., Baker, D. M., and Lesser, M. P. (2013). Nitrogen biogeochemistry in the caribbean sponge, *Xestospongia muta*: a source or sink of dissolved inorganic nitrogen? *PLoS ONE* 8:72961. doi: 10.1371/journal.pone.0072961

Francis, C. A., Roberts, K. J., Beman, J. M., Santoro, A. E., and Oakley, B. B. (2005). Ubiquity and diversity of ammonia-oxidizing archaea in water columns and sediments of the ocean. *Proc. Natl. Acad. Sci. U. S. A.* 102, 14683–14688. doi: 10.1073/pnas.0506625102

Fristedt, K. (1887). Sponges from the Atlantic and Arctic Oceans and the Behring Sea. Vega-Expeditionens Vetenskap. *Iakttag.* 4, 401–471.

Gage, J. D., and Tyler, P. A. (1991). *Deep-Sea Biology: A Natural History of Organisms at the Deep-Sea Floor*. Cambridge: Cambridge University Press. doi: 10.1017/CBO9781139163637

Gili, J.-M., and Coma, R. (1998). Benthic suspension feeders: their paramount role in littoral marine food webs. *Trends Ecol. Evol.* 13, 316–321. doi: 10.1016/S0169-5347(98)01365-2

Hancock, J. T. (2017). *Cell Signalling, 4th Edn*. Oxford: Oxford University Press.

Hawkes, N., Korabik, M., Beazley, L., Rapp, H. T., Xavier, J. R., and Kenchington, E. (2019). Glass sponge grounds on the Scotian Shelf and their associated biodiversity. *Mar. Ecol. Prog. Ser.* 614, 91–109. doi: 10.3354/meps12903

Hoer, D. R., Tommerdahl, J. P., Lindquist, N. L., and Martens, C. S. (2018). Dissolved inorganic nitrogen fluxes from common Florida Bay (U.S.A.) sponges. *Limnol. Oceanogr.* 63, 2563–2578. doi: 10.1002/lno.10960

Hoffmann, F., Radax, R., Woebken, D., Holtappels, M., Lavik, G., Rapp, H. T., et al. (2009). Complex nitrogen cycling in the sponge *Geodia barretti*. *Environ. Microbiol.* 11, 2228–2243. doi: 10.1111/j.1462-2920.2009.01944.x

Jiménez, E., and Ribes, M. (2007). Sponges as a source of dissolved inorganic nitrogen: nitrification mediated by temperate sponges. *Limnol. Oceanogr.* 52, 948–958. doi: 10.4319/lo.2007.52.3.0948

Jones, P., Binns, D., Chang, H. Y., Fraser, M., Li, W., McAnulla, C., et al. (2014). InterProScan 5: genome-scale protein function classification. *Bioinformatics* 30, 1236–1240. doi: 10.1093/bioinformatics/btu031

Kahn, A. S., Chu, J. W. F., and Leys, S. P. (2018). Trophic ecology of glass sponge reefs in the Strait of Georgia, British Columbia. *Sci. Rep.* 8:756. doi: 10.1038/s41598-017-19107-x

Keesing, J. K., Strzelecki, J., Fromont, J., and Thomson, D. (2013). Sponges as important sources of nitrate on an oligotrophic continental shelf. *Limnol. Oceanogr.* 58, 1947–1958. doi: 10.4319/lo.2013.58.6.1947

Kimmerer, W. J., Gartside, E., and Orsi, J. (1994). Predation by an introduced clam as the likely cause of substantial declines in zooplankton of San Francisco Bay. *Mar. Ecol. Prog. Ser.* 1113, 81–93. doi: 10.3354/meps113081

Kitzinger, K., Marchant, H. K., Bristow, L. A., Herbold, C. W., Padilla, C. C., Kidane, A. T., et al. (2020). Single cell analyses reveal contrasting life strategies of the two main nitrifiers in the ocean. *Nat. Commun.* 11:3. doi: 10.1038/s41467-020-14542-3

Klawonn, I., Bonaglia, S., Whitehouse, M. J., Littmann, S., Tienken, D., Kuypers, M. M. M., et al. (2019). Untangling hidden nutrient dynamics: rapid ammonium cycling and single-cell ammonium assimilation in marine plankton communities. *ISME J.* 13, 1960–1974. doi: 10.1038/s41396-019-0386-z

Leys, S. P., Kahn, A. S., Fang, J. K. H., Kutti, T., and Bannister, R. J. (2017). Phagocytosis of microbial symbionts balances the carbon and nitrogen budget for the deep-water boreal sponge *Geodia barretti*. *Limnol. Oceanogr.* 63, 187–202. doi: 10.1002/lno.10623

Li, D., Luo, R., Liu, C. M., Leung, C. M., Ting, H. F., Sadakane, K., et al. (2016). MEGAHIT v1.0: a fast and scalable metagenome assembler driven by advanced methodologies and community practices. *Methods* 102, 3–11. doi: 10.1016/j.ymeth.2016.02.020

López-Acosta, M., Leynaert, A., Chavaud, L., Amice, E., Bihannic, I., Le Bec, T., et al. (2019). In situ determination of Si, N, and P utilization by the demosponge *Tethya citrina*: a benthic-chamber approach. *PLoS ONE* 14:218787. doi: 10.1371/journal.pone.0218787

Lozupone, C., Lladser, M. E., Knights, D., Stombaugh, J., and Knight, R. (2011). UniFrac: an effective distance metric for microbial community comparison. *ISME J.* 5, 169–172. doi: 10.1038/ismej.2010.133

Mackie, G. O., and Singla, C. L. (1983). Studies on hexactinellid sponges. I. Histology of *Rhabdocalyptus dawsoni* (Lambe, 1873). *Philos. Trans. R. Soc. London* 301, 365–400. doi: 10.1098/rstb.1983.0028

Maldonado, M. (2007). Intergenerational transmission of symbiotic bacteria in oviparous and viviparous demosponges, with emphasis on intracytoplasmically-compartmented bacterial types. *J. Mar. Biol. Assoc. United Kingdom* 87, 1701–1713. doi: 10.1017/S0025315407058080

Maldonado, M. (2015). Sponge waste that fuels marine oligotrophic food webs: a re-assessment of its origin and nature. *Mar. Ecol.* 37, 1–15. doi: 10.1111/maec.12256

Maldonado, M., Aguilar, R., Bannister, R. J., Bell, J. J., Conway, K. W., Dayton, P. K., et al. (2017). "Sponge grounds as key marine habitats: a synthetic review of types, structure, functional roles, and conservation concerns," in *Marine Animal Forests: The Ecology of Benthic Biodiversity Hotspots*, eds L. Sergio Rossi, A. Bramanti, A. Gori, and C. Orejas (Cham, Switzerland: Springer International Publishing), 145–183.

Maldonado, M., Beazley, L., López-Acosta, M., Kenchington, E., Casault, B., Hanz, U., et al. (2021). Massive silicon utilization facilitated by a benthic-pelagic coupled feedback sustains deep-sea sponge aggregations. *Limnol. Oceanogr.* 66, 366–391. doi: 10.1002/lno.11610

Maldonado, M., López-Acosta, M., Beazley, L., Kenchington, E., Koutsouveli, V., and Riesgo, A. (2020). Cooperation between passive and active silicon transporters clarifies the ecophysiology and evolution of biosilicification in sponges. *Sci. Adv.* 6:eaba9322. doi: 10.1126/sciadv.aba9322

Maldonado, M., Ribes, M., and van Duyl, F. C. (2012). Nutrient fluxes through sponges. Biology, budgets, and ecological implications. *Adv. Mar. Biol.* 62, 113–182. doi: 10.1016/B978-0-12-394283-8.00003-5

Mohamed, N. M., Tal, Y., and Hill, R. T. (2008). Diversity and expression of nitrogen fixation genes in bacterial symbionts of marine sponges. *Environ. Microbiol.* 10, 2910–2921. doi: 10.1111/j.1462-2920.2008.01704.x

Moitinho-Silva, L., Nielsen, S., Amir, A., Gonzalez, A., Ackermann, G. L., Cerrano, C., et al. (2017). The sponge microbiome project. *Gigascience* 6, 1–7. doi: 10.1093/gigascience/gix077

Morganti, T., Coma, R., Yahel, G., and Ribes, M. (2017). Trophic niche separation that facilitates co-existence of high and low microbial abundance sponges is revealed by *in situ* study of carbon and

nitrogen fluxes. *Limnol. Oceanogr.* 62, 1963–1983. doi: 10.1002/lno.10546

Nelson, C. E., Alldredge, A. L., McCliment, E. A., Amaral-Zettler, L. A., and Carlson, C. A. (2011). Depleted dissolved organic carbon and distinct bacterial communities in the water column of a rapid-flushing coral reef ecosystem. *ISME J.* 5, 1374–1387. doi: 10.1038/ismej.2011.12

Petrie, B., Yeats, P., Strain, P., and Services, M., of S. and (1999). *Nitrate, silicate and phosphate atlas for the Scotian shelf and the gulf of Maine*. Dartmouth, NS: Fisheries and Oceans Canada.

Pile, A. J., and Young, C. M. (2006). The natural diet of a hexactinellid sponge: benthic-pelagic coupling in a deep-sea microbial food web. *Deep. Res. Part I Oceanogr. Res. Pap.* 53, 1148–1156. doi: 10.1016/j.dsr.2006.03.008

Pita, L., Rix, L., Slaby, B. M., Franke, A., and Hentschel, U. (2018). The sponge holobiont in a changing ocean: from microbes to ecosystems. *Microbiome* 6:46. doi: 10.1186/s40168-018-0428-1

Price, M. N., Dehal, P. S., and Arkin, A. P. (2010). FastTree 2 - approximately maximum-likelihood trees for large alignments. *PLoS ONE* 5:e9490. doi: 10.1371/journal.pone.0009490

Quast, C., Pruesse, E., Yilmaz, P., Gerken, J., Schweer, T., Yarza, P., et al. (2013). The SILVA ribosomal RNA gene database project: improved data processing and web-based tools. *Nucl. Acids Res.* 41:D590. doi: 10.1093/nar/gks1219

Quin, L. D. (2000). *A Guide to Organophosphorus*. New York, NY: Wiley-Interscience.

Radax, R., Hoffmann, F., Rapp, H. T., Leininger, S., and Schleper, C. (2012). Ammonia-oxidizing archaea as main drivers of nitrification in cold-water sponges. *Environ. Microbiol.* 14, 909–923. doi: 10.1111/j.1462-2920.2011.02661.x

Ribes, M., Dziallas, C., Coma, R., and Riemann, L. (2015). Microbial diversity and putative diazotrophy in high- and low- microbial-abundance mediterranean sponges. *Appl. Environ. Microbiol.* 81, 5683–5693. doi: 10.1128/AEM.01320-15

Ribes, M., Jiménez, E., Yahel, G., López-Sendino, P., Diez, B., Massana, R., et al. (2012). Functional convergence of microbes associated with temperate marine sponges. *Environ. Microbiol.* 14, 1224–1239. doi: 10.1111/j.1462-2920.2012.02701.x

Rix, L., Ribes, M., Coma, R., Martin, J.ahn, T., and De Goeij, J. M., Dick Van Oevelen, et al. (2020). Heterotrophy in the earliest gut: a single-cell view of heterotrophic carbon and nitrogen assimilation in sponge-microbe symbioses. *ISME J.* 14, 2554–2567. doi: 10.1038/s41396-020-0706-3

Rooks, C., Kar-Hei Fang, J., Mørkved, P. T., Zhao, R., Tore Rapp, H., Xavier, J. J., et al. (2020). Deep-sea sponge grounds as nutrient sinks: denitrification is common in boreo-Arctic sponges. *Biogeosciences* 17, 1231–1245. doi: 10.5194/bg-17-1231-2020

Sangrador-Vegas, A., Mitchell, A. L., Chang, H. Y., Yong, S. Y., and Finn, R. D. (2016). GO annotation in InterPro: why stability does not indicate accuracy in a sea of changing annotations. *Database* 2016:baw027. doi: 10.1093/database/baw027

Scheffers, S. R., Nieuwland, G., Bak, R. P. M., and Van Duyl, F. C. (2004). Removal of bacteria and nutrient dynamics within the coral reef framework of Curacao (Netherlands Antilles). *Coral Reefs* 23, 413–422. doi: 10.1007/s00338-004-0400-3

Schläppy, M.-L., Schöttner, S. I., Lavik, G., Kuypers, M. M. M., de Beer, D., and Hoffmann, F. (2010). Evidence of nitrification and denitrification in high and low microbial abundance sponges. *Mar. Biol.* 157, 593–602. doi: 10.1007/s00227-009-1344-5

Schmidt, O. (1870). *Grundzüge einer Spongien-Fauna des Atlantischen Gebietes*. Leipzing: Wilhelm Engelmann, 1–88.

Segata, N., Izard, J., Waldron, L., Gevers, D., Miropolsky, L., Garrett, W. S., et al. (2011). Metagenomic biomarker discovery and explanation. *Genome Biol.* 12:R60. doi: 10.1186/gb-2011-12-6-r60

Smith, S. V. (1984). Phosphorus versus nitrogen limitation in the marine environment. *Limnol. Oceanogr.* 29, 1149–1160. doi: 10.4319/lo.1984.29.6.1149

Southwell, M. W., Popp, B. N., and Martens, C. S. (2008a). Nitrification controls on fluxes and isotopic composition of nitrate from Florida Keys sponges. *Mar. Chem.* 108, 96–108. doi: 10.1016/j.marchem.2007.10.005

Southwell, M. W., Weisz, J. B., Martens, C. S., and Lindquist, N. (2008b). *In situ* fluxes of dissolved inorganic nitrogen from the sponge community on Conch Reef, Key Largo, Florida. *Limnol. Oceanogr. Methods* 53, 986–996. doi: 10.4319/lo.2008.53.3.0986

Steinert, G., Busch, K., Bayer, K., Kodami, S., Arbizu, P. M., Kelly, M., et al. (2020). Compositional and quantitative insights into bacterial and archaeal communities of South Pacific Deep-Sea Sponges (Demospongiae and Hexactinellida). *Front. Microbiol.* 11:716. doi: 10.3389/fmicb.2020.00716

Strickland, J. D. H., and Parsons, T. R. (1972). *A practical handbook of seawater analysis, 2nd Edn*. Ottawa, ON: Fisheries Research Board of Canada.

Subina, N. S., Thorat, B. R., and Gonsalves, M.-J. (2018). Nitrification in intertidal sponge *Cinachyrella cavernosa*. *Aquat. Ecol.* 52, 155–164. doi: 10.1007/s10452-018-9651-x

Tabachnick, K. R. (1994). "Distribution of recent Hexactinellida," in *Sponges in Time and Space*, eds. R. M. W. van Soest, T. M. G. van Kempen, and J. C. Braekman (Rotterdam: A.A. Balkema), 225–232.

Ternan, N. G., Mc Grath, J. W., Mc Mullan, G., and Quinn, J. P. (1998). Review: organophosphonates: occurrence, synthesis and biodegradation by microorganisms. *World J. Microbiol. Biotechnol.* 14, 635–647. doi: 10.1023/A:1008848401799

Thomas, T., Moitinho-Silva, L., Lurgi, M., Björk, J. R., Easson, C., Astudillo-García, C., et al. (2016). Diversity, structure and convergent evolution of the global sponge microbiome. *Nat. Commun.* 7:11870. doi: 10.1038/ncomms11870

Tian, R. M., Sun, J., Cai, L., Zhang, W. P., Zhou, G. W., Qiu, J. W., et al. (2016). The deep-sea glass sponge Lophophysema eversa harbours potential symbionts responsible for the nutrient conversions of carbon, nitrogen and sulfur. *Environ. Microbiol.* 18, 2481–2494. doi: 10.1111/1462-2920.13161

Uritskiy, G. V., Diruggiero, J., and Taylor, J. (2018). MetaWRAP - A flexible pipeline for genome-resolved metagenomic data analysis 08 Information and Computing Sciences 0803 Computer Software 08 Information and Computing Sciences 0806 Information Systems. *Microbiome* 6:158. doi: 10.1186/s40168-018-0541-1

Vacelet, J., Boury-Esnault, N., and Harmelin, J. G. (1994). Hexactinellid Cave, a unique deep-sea habitat in the scuba zone. *Deep. Res. I* 41, 965–973. doi: 10.1016/0967-0637(94)90013-2

Van Duyl, F. C., Hegeman, J., Hoogstraten, A., and Maier, C. (2008). Dissolved carbon fixation by sponge–microbe consortia of deep water coral mounds in the northeastern Atlantic Ocean. *Mar. Ecol. Prog. Ser.* 358, 137–150. doi: 10.3354/meps07370

Villarreal-Chiu, J. F., Quinn, J. P., and McGrath, J. W. (2012). The genes and enzymes of phosphonate metabolism by bacteria, and their distribution in the marine environment. *Front. Microbiol.* 3. doi: 10.3389/fmicb.2012.00019

White, A. K., and Metcalf, W. W. (2007). Microbial metabolism of reduced phosphorus compounds. *Annu. Rev. Microbiol.* 61, 379–400. doi: 10.1146/annurev.micro.61.080706.093357

Wilkinson, C. R., and Fay, P. (1979). Nitrogen fixation in coral reef sponges with symbiotic cyanobacteria. *Nature* 279, 527–529. doi: 10.1038/279527a0

Wilkinson, C. R., Summons, R. E., and Evans, E. (1999). Nitrogen fixation in symbiotic marine sponges: ecological significance and difficulties in detection. *Mem. Queensl. Museum* 44, 667–673.

Wuchter, C., Abbas, B., Coolen, M. J. L., Herfort, L., van Bleijswijk, J., Timmers, P., et al. (2006). Archaeal nitrification in the ocean. *Proc. Natl. Acad. Sci. U. S. A.* 103, 12317–12322. doi: 10.1073/pnas.0600756103

Yahel, G., Whitney, F., Reiswig, H. M., Eerkes-Medrano, D. I., and Leys, S. P. (2007). *In situ* feeding and metabolism of glass sponges (Hexactinellida, Porifera) studied in a deep temperate fjord with a remotely operated submersible. *Limnol. Oceanogr.* 52, 428–440. doi: 10.4319/lo.2007.52.1.0428

Zakem, E. J., Al-Haj, A., Church, M. J., Van Dijken, G. L., Dutkiewicz, S., Foster, S. Q., et al. (2018). Ecological control of nitrite in the upper ocean. *Nat. Commun.* 9, 1–13. doi: 10.1038/s41467-018-03553-w

Zhang, F., Jonas, L., Lin, H., and Hill, R. T. (2019). Microbially mediated nutrient cycles in marine sponges. *FEMS Microbiol. Ecol.* 95. doi: 10.1093/femsec/fiz155

**Conflict of Interest:** The authors declare that the research was conducted in the absence of any commercial or financial relationships that could be construed as a potential conflict of interest.

# *Supplementary Material*

**CONTENTS**



**SUPPLEMENTARY VIDEO 1|** Digital video showing the sponge-dominate benthic community at the Arctic Schulz Bank seamount as recorded by the AEGIR 6000 ROV during a dive aimed to deploy the incubation chambers. Note the abundance of *Schaudinnia rosea*, which are the white tubular sponges.

**SUPPLEMENTARY VIDEO 2|** Digital video showing the monospecific aggregation of *Vazella pourtalesii* at Sambro Bank Sponge Conservation Area on the Nova Scotia Shelf, Canada, as recorded by the ROPOS ROV.

**SUPPLEMENTARY VIDEO 3|** Video showing the incubation of an individual of *Schaudinnid rosea* at the Arctic Schulz Bank seamount as recorded by the AEGIR 6000 ROV.

**SUPPLEMENTARY VIDEO 4|** Video showing the incubation of an individual of *Vazella pourtalaesii* at Sambro Bank Sponge Conservation Area on the Nova Scotia Shelf, Canada, as recorded by the ROPOS ROV.

**SUPPLEMENTARY DATA FILE 1|** Excel file containing the triangular matrix of Weighted UniFrac distances between pairs of samples, including tissue of *Schaudinnia rosea* and *Vazella pourtalesii*, and seawater from their respective habitats. Distances resulted from the taxonomic classification of Amplicon Sequence Variants (ASVs) performed using a Bayes classifier and were calculated based on a phylogeny produced with FastTree2. Distances were then submitted to the non-metric multidimensional scaling to produce the ordination space of **Figure 5**.

**SUPPLEMENTARY DATA FILE 2|** Excel data file containing the calculations of the annual net nutrient flux across the aggregations of *Vazella pourtalesii*.

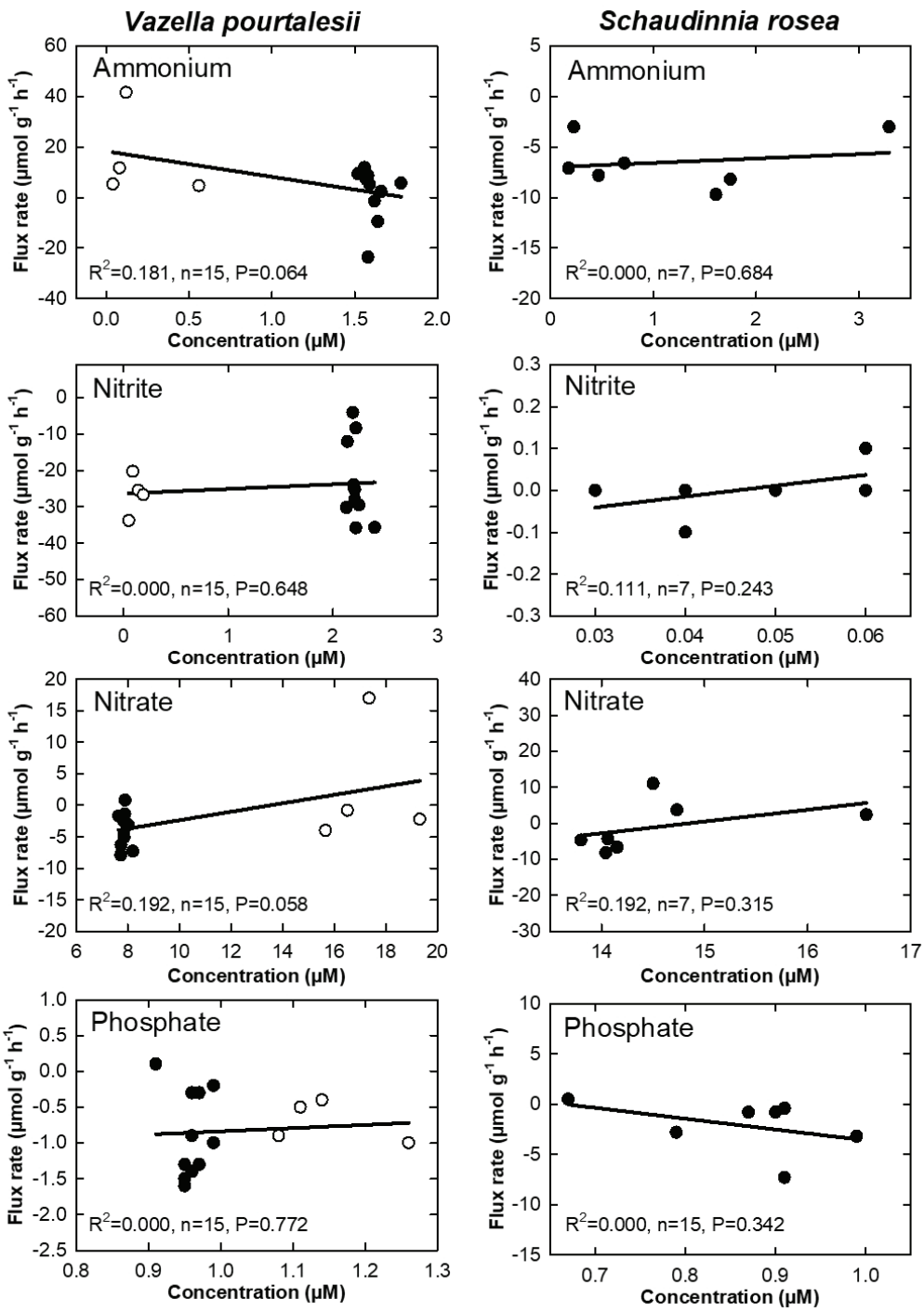


`

**SUPPLEMENTARY FIGURE 1 |** Linear regression analysis examining nutrient flux rates as a function of ambient nutrient concentration for the two assayed sponge species. In *Vazella pourtalesii*, in-situ incubations (open circles) were combined with 1st day laboratory incubations (solid circles) for the analyses. Note that the relationship lacks statistical significance in all cases ($P > 0.05$) and that the strength of the association between the two variables is consistently very low (adjusted $R^2 < 0.2$).

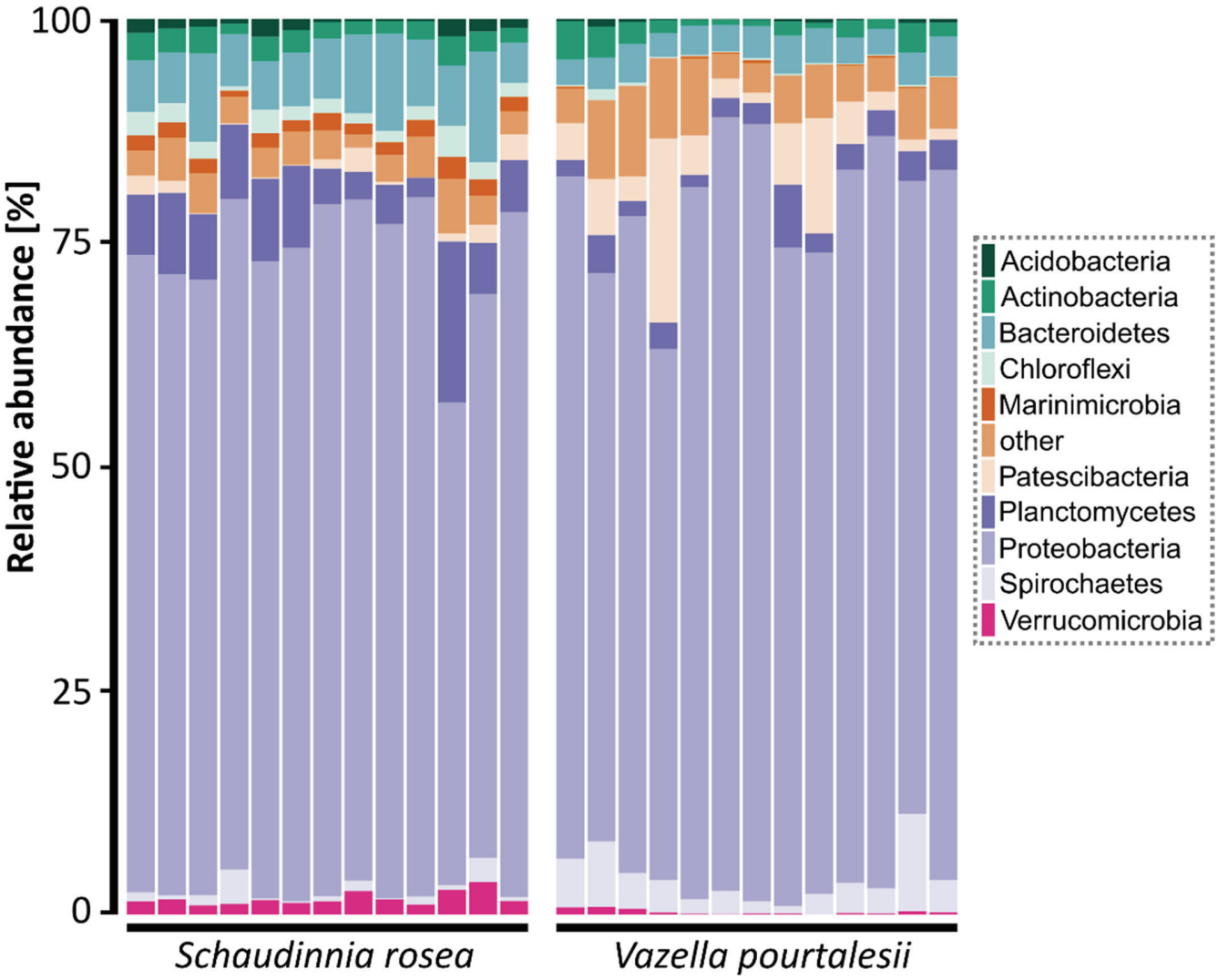


**SUPPLEMENTARY FIGURE 2 |** Summary of relative abundances in the composition of the microbiomes (at the phylum level) of *Schaudinnia rosea* and *Vazella pourtalesii*. The ten most abundant phyla are displayed, while the remaining, low-abundance phyla are combined under the category "other". Additional information on the microbiomes of these sponge species can be found somewhere else (Bayer et al., 2020; Busch et al., 2020b, 2020a).

**SUPPLEMENTARY TABLE 1 |** Summary of tests examining differences in the flux rate of nutrients (ammonium, nitrite, nitrate, phosphate) in *Vazella pourtalesii* as function of rates having been through an *in-situ* incubation or a laboratory incubation. Note that ammonium, nitrite and phosphate results made normal and homoscedastic data sets suitable for the parametric *t*-test. The non-normal and heteroscedastic data of nitrate were analyzed through the non-parametric Mann-Whitney *U* test. In no case, there were statistically significant differences between incubation modes. Therefore, result from both incubation modes were pooled together to extract global average values. "N", "Mean" and "SD" indicate, respectively, the number of replicates per incubation mode, along with its average value and standard deviation. "*p*" indicates the statistical significance of each pairwise comparison test.

| **Nutrient** | **N** | **Mean** | **SD** | **Statistic type** | **Statistic value** | ***p*** |
|---|---|---|---|---|---|---|
| Ammonium | | | | | | |
| in situ | 4 | 15.8 | 17.4 | *t*-test | -1.858 | 0.086 |
| ex situ | 11 | 2.3 | 10.5 | | | |
| Nitrite | | | | | | |
| in situ | 4 | -26.6 | 5.6 | *t*-test | 0.554 | 0.589 |
| ex situ | 11 | -23.4 | 10.7 | | | |
| Nitrate * | | | | | | |
| in situ | 4 | 2.5 | 9.7 | *U*-test | 10.000 | 0.133 |
| ex situ | 11 | -3.8 | 2.7 | | | |
| Phosphate | | | | | | |
| in situ | 4 | -0.7 | 0.3 | *t*-test | -0.551 | 0.591 |
| ex situ | 11 | -0.9 | 0.6 | | | |

**SUPPLEMENTARY TABLE 2** | Summary of net fluxes of $NH_4^+$ over the seven consecutive laboratory incubations of eleven *Vazella pourtalesii* individuals (Ind. codes #5 to #15). The ambient ammonium concentration (µM) at the beginning of each incubation is given on the left-hand section of the table and the measured net flux rate ($10^{-3}$ µmol of ammonium per sponge mL and hour) in the right-hand section. Note that individuals 1-4 are missing from the table, because they were incubated *in situ* but not in the laboratory. The mean (AVG) value of each incubation step and its associated standard deviation (SD) are given at the two bottom rows of the table.

| Ind. code | Ambient $NH_4^+$ (µM) | | | | | | | $NH_4^+$ flux rate ($10^{-3}$ µmol $mL^{-1}$ $h^{-1}$) | | | | | | |
|---|---|---|---|---|---|---|---|---|---|---|---|---|---|---|
| | Incubation step | | | | | | | Incubation step | | | | | | |
| | 1 | 2 | 3 | 4 | 5 | 6 | 7 | 1 | 2 | 3 | 4 | 5 | 6 | 7 |
| **5** | 1.5 | 2.1 | 1.6 | 0.3 | 0.6 | 0.3 | 1.5 | 9.4 | 8.5 | 3.1 | 3.4 | -1.2 | -1.3 | 2.5 |
| **6** | 1.6 | 2.0 | 1.6 | 0.5 | 0.7 | 0.5 | 1.6 | 7.2 | 7.0 | 0.1 | -6.4 | -2.2 | -5.5 | -5.3 |
| **7** | 1.6 | 2.3 | 1.7 | 0.3 | 0.7 | 0.5 | 1.5 | -1.4 | 5.8 | 1.6 | -4.0 | -1.2 | -5.6 | -3.0 |
| **8** | 1.6 | 1.6 | 1.6 | 0.0 | 0.6 | 0.5 | 1.4 | 9.4 | 11.4 | 2.4 | 0.6 | 3.0 | 4.0 | 7.5 |
| **9** | 1.6 | 2.0 | 1.7 | 0.3 | 0.7 | 0.5 | 1.5 | -9.5 | -16.0 | -6.1 | -6.1 | -7.6 | -14.7 | -6.2 |
| **10** | 1.8 | 2.0 | 1.5 | 0.3 | 0.6 | 0.4 | 1.4 | 5.7 | 13.8 | 9.0 | 4.1 | -1.0 | -5.5 | 3.0 |
| **11** | 1.6 | 2.0 | 1.5 | 0.4 | 0.6 | 0.5 | 1.5 | 11.9 | 17.4 | 2.5 | -5.9 | -2.9 | -2.7 | -3.4 |
| **12** | 1.6 | 2.0 | 1.5 | 0.4 | 0.5 | 0.5 | 1.5 | 8.7 | 12.1 | -4.7 | -6.1 | -8.0 | -12.3 | -11.8 |
| **13** | 1.6 | 2.2 | 1.6 | 0.4 | 0.6 | 0.4 | 1.4 | -23.6 | -20.0 | -24.5 | -18.3 | -19.4 | -24.4 | -18.7 |
| **14** | 1.7 | 2.0 | 1.6 | 0.4 | 0.6 | 0.4 | 1.4 | 2.4 | -5.9 | -0.3 | -6.0 | -6.5 | -7.7 | -7.5 |
| **15** | 1.6 | 2.1 | 1.7 | 0.5 | 0.6 | 0.4 | 1.4 | 5.2 | 0.2 | -6.4 | -5.5 | -10.9 | -13.0 | -6.7 |
| **AVRG** | 1.6 | 2.0 | 1.6 | 0.3 | 0.6 | 0.5 | 1.5 | 2.3 | 3.1 | -2.1 | -4.6 | -5.2 | -8.1 | -4.5 |
| **SD** | 0.1 | 0.2 | 0.1 | 0.1 | 0.0 | 0.1 | 0.1 | 10.5 | 12.3 | 8.7 | 6.1 | 6.2 | 7.7 | 7.2 |

**SUPPLEMENTARY TABLE 3** | Summary of PERMANOVA tests showing the statistical significance of the groups of samples identified by a nMDS analysis (**Figure 5**) based on between-sample UniFrac distances obtained for the amplicon data.

| Group 1 | Group 2 | Sample size | Permutations | pseudo-F | p-value |
|---|---|---|---|---|---|
| *Schaudinnia rosea* | *Vazella pourtalesii* | 26 | 999 | 40.9 | 0.001 |
| *Schaudinnia rosea* | seawater *Schaudinnia rosea* | 19 | 999 | 16.3 | 0.001 |
| *Vazella pourtalesii* | seawater *Vazella pourtalesii* | 16 | 999 | 30.2 | 0.002 |

**SUPPLEMENTARY TABLE 4** | Genes encoding for enzymes involved in microbial nitrogen **(A)** cycle and phosphonate catabolism **(B)** detected in the microbiome of the sponge *Vazella pourtalesii*. The metagenome assembled genomes (MAGs) and their respective phylogenetic affiliations are given, following Bayer et al. (2020). Bold writing indicates MAGs that were enriched in the sponge over seawater. Enzymes missing in the MAGs are indicated by a dash (**-**) and enzymes found in the unbinned data are indicated by an asterisk (*).

| (A) Pathway | Enzymes | EC | K term | Reaction | MAGs | Phylogenetic affiliation |
|---|---|---|---|---|---|---|
| Nitrification | ammonia monooxygenase (*amoABC*) | 1.14.99.39 | K10944, K10945, K10946 | $NH_3^+$ → $NH_2OH$ | **74, 90, 143**<br>131<br>46 | **Crenarchaeota**<br>Crenarchaeota<br>Gammaproteobacteria |
| | hydroxylamine dehydrogenase (*hao*) | 1.7.2.6 | K10535 | $NH_2OH$ → $NO_2^-$ | | * |
| | nitrite oxidoreductase (*nxrA*) | 1.7.99.- | K00370 | $NO_2^-$ → $NO_3^{2-}$ | | - |
| Denitrification | nitrate reductase (*narG, narH, narJ*) | 1.7.5.1 | K00370, K00371, K00374 | $NO_3^{2-}$ → $NO_2^-$ | **70**<br>**64** | **Alphaproteobacteria**<br>**Actinobacteriota** |
| | nitrate reductase (cytochrome) (*napA, napB*) | 1.9.6.1 | K02567, K02568 | $NO_3^{2-}$ → $NO_2^-$ | **52** | **Planctomycetota** |
| | nitrite reductase (NO-forming) (*nirK, nirS*) | 1.7.2.1 | K00368, K15864 | $NO_2^-$ → NO | **90, 143**<br>36, 101, 131<br>86 | **Crenarchaeota**<br>Crenarchaeota<br>Acidobacteriota |
| | nitric oxide reductase (*norB, norC*) | 1.7.2.5 | K04561, K02305 | NO → $N_2O$ | | - |
| | nitrous-oxide reductase (*nosZ*) | 1.7.2.4 | K00376 | $N_2O$ → $N_2$ | | * |
| Dissimilatory nitrate reduction | nitrate reductase (*narG, narH, narJ*) | 1.7.5.1 | K00370, K00371, K00374 | $NO_3^{2-}$ → $NO_2^-$ | **70**<br>**64** | **Alphaproteobacteria**<br>**Actinobacteriota** |
| | nitrate reductase (cytochrome) (*napA, napB*) | 1.9.6.1 | K02567, K02568 | $NO_3^{2-}$ → $NO_2^-$ | **52** | **Planctomycetota** |
| | nitrite reductase (cytochrome c-552) (*nrfA, nrfH*) | 1.7.2.2 | K03385, K15876 | $NO_2^-$ → $NH_3^+$ | | * |

| | | | | | | |
|---|---|---|---|---|---|---|
| | nitrite reductase (NADH) (*nirB, nirD*) | 1.7.1.15 | K00362, K00363 | $NO_2^- \rightarrow NH_3^+$ | **52, 99**<br>**64**<br>89 | **Planctomycetota**<br>**Actinobacteriota**<br>Gammaproteobacteria |
| Nitrogen fixation | nitrogenase molybdenum-iron protein (*nifD, nifK, nifH, anfG*) | 1.18.6.1 | K02586, K02591, K02588, K00531 | $N_2 \rightarrow NH_3^+$ | **88**<br>**91**<br>77, 127<br>24<br>135 | **Firmicutes**<br>**Planctomycetota**<br>Firmicutes<br>Bacteroidota<br>Alphaproteobacteria |
| other | hydroxylamine reductase (*hcp)* | 1.7.99.1 | K05601 | $NH_2OH \rightarrow NH_3^+$ | **119**<br>127 | **Planctomycetota**<br>Firmicutes |
| Assimilation | glutamate dehydrogease (*gudB, rocG*) | 1.4.1.2 | K00260, K15371 | $NH_3^+ + C_5H_6O_5 \rightarrow C_5H_9NO_4$ | **27, 50, 58, 65, 70, 96, 104, 109, 114, 118**<br>**10, 34, 51, 108, 137**<br>**56**<br>**74, 90, 143**<br>**75, 94, 132**<br>**8, 126, 140**<br>**64**<br>**105**<br>141<br>63, 89<br>67, 110<br>13 | **Alphaproteobacteria**<br>**Gammaproteobacteria**<br>**Spirochaetota**<br>**Crenarchaeota**<br>**Planctomycetota**<br>**SAR324**<br>**Actinobacteriota**<br>**Verrucomicrobiota**<br>Alphaproteobacteria<br>Gammaproteobacteria<br>Planctomycetota<br>Myxococcota |

| | | | | | | |
|---|---|---|---|---|---|---|
| | glutamine synthetase (*glnA, GLUL*) | 6.3.1.2 | K01915 | $NH_3^+ + C_5H_9NO_4 \rightarrow C_5H_{10}N_2O_3$ | **19, 21, 27, 50, 58, 65, 70, 96, 104, 109, 118** | **Alphaproteobacteria** |
| | | | | | **4, 9, 10, 34, 40, 51, 58, 139** | **Gammaproteobacteria** |
| | | | | | **56, 91, 93, 94, 125** | **Spirochaetota** |
| | | | | | **32, 52, 61, 75, 91, 113, 116, 119, 121, 132, 134** | **Planctomycetota** |
| | | | | | **8, 126, 140** | **SAR324** |
| | | | | | **64, 80, 111** | **Actinobacteriota** |
| | | | | | **6, 22** | **Myxococcota** |
| | | | | | **74, 143** | **Crenarchaeota** |
| | | | | | **3, 28** | **Bacteroidota** |
| | | | | | 42, 71, 115, 124, 135, 141 | Alphaproteobacteria |
| | | | | | 47, 53, 94, 97, 100, 123 | Chloroflexota |
| | | | | | 26, 66, 111 | Actinobacteriota |
| | | | | | 44, 55, 87, 92, 124, 142 | Firmicutes |
| | | | | | 1, 2, 7, 24, 49, 54, 60, 87 | Bacteroidota |
| | | | | | 35, 45, 46, 63, 69, 89 | Gammaproteobacteria |
| | | | | | 72 | Acidobacteriota |
| | | | | | 59, 67, 110, 121 | Planctomycetota |
| | | | | | 11, 15, 18, 107, 133 | Thermoplasmatota |
| | | | | | 36, 101, 131 | Crenarchaeota |
| | | | | | 14, 37, 68 | Marinisomatota |
| | | | | | 23, 84, 85, 112 | Verrucomicrobiota |

| (B) Pathway | Enzymes | EC | K term | Reaction | MAG(s) | Phylogenetic affiliation |
|---|---|---|---|---|---|---|
| C-P lyase pathway | ABC transporter (*phnCDE*) | 7.3.2.2<br>TC: 3.A.1.9 | K02041, K02044, K02042 | uptake | **22** | **Myxococcota** |
| | | | | | **74, 143** | **Crenarchaeota** |
| | | | | | 15, 83, 107, 117, 130 | Thermoplasmatota |
| | | | | | 112 | Verrucomicrobiota |
| | | | | | 36, 101 | Crenarchaeota |
| | | | | | 17, 111 | Actinobacteriota |
| | | | | | 17, 49 | Bacteroidota |
| | | | | | 124 | Alphaproteobacteria |
| | | | | | 100 | Chloroflexota |
| | C-P lyase (*phnGHIJKLM*) | 4.7.1.1 | K06163 | C-P bond cleavage | 124 | Alphaproteobacteria * |
| | related to C–P lyase: DUF1045 | | | | 124, 135 | Alphaproteobacteria |
| 2-aminoethylphosphonate (2AEP) catabolism | 2-aminoethylphosphonate-pyruvate transaminase, pyruvate aminotransferase (*phnW*) | 2.6.1.37 | K03430 | 2AEP + Pyruvate <=> Phosphonoacetaldehyde + L-Alanine | **52, 94, 116, 119** | **Planctomycetota** |
| | | | | | **74, 90, 143** | **Crenarchaeota** |
| | | | | | **75** | **Alphaproteobacteria** |
| | | | | | **10** | **Gammaproteobacteria** |
| | | | | | 124, 135, 141 | Alphaproteobacteria |
| | | | | | 47, 53 | Chloroflexota |
| | | | | | 123, 131 | Crenarchaeota |
| | | | | | 9, 35, 63, 89 | Gammaproteobacteria |
| | | | | | 59 | Myxococcota |
| | | | | | 44 | Firmicutes |
| | | | | | 15, 83 | Thermoplasmatota |
| | | | | | 86 | Acidobacteriota |
| | | | | | 23, 84, 112 | Verrucomicrobiota |
| | | | | | 37, 82 | Marinisomatota |
| | | | | | 24 | Bacteroidota |

| | | | | | | |
|---|---|---|---|---|---|---|
| | phosphonoacetaldehyde hydrolase, phosphonatase (*phnX*) | 3.11.1.1 | K05306 | Phosphonoacetaldehyde <=> Acetaldehyde + Pi | **52, 119** | **Planctomycetota** |
| other | phosphonoacetate hydrolase (*phnA*) | 3.11.1.2 | K19670 | Phosphonoacetate + H2O <=> Acetate + Orthophosphate | **121**<br>59<br>124, 135<br>75<br>63<br>23, 85, 112 | **Planctomycetota**<br>Myxococcota<br>Alphaproteobacteria<br>Planctomycetota<br>Gammaproteobacteria<br>Verrucomicrobiota |

## REFERENCES

Bayer, K., Busch, K., Kenchington, E., Beazley, L., Franzenburg, S., Michels, J., et al. (2020). Microbial strategies for survival in the glass sponge Vazella pourtalesii. *mSystems* 5, e00473-20. doi:10.1128/mSystems.00473-20.

Busch, K., Beazley, L., Kenchington, E., Whoriskey, F., Slaby, B. M., and Hentschel, U. (2020a). Microbial diversity of the glass sponge Vazella pourtalesii in response to anthropogenic activities. *Conserv. Genet.* 21, 1001–1010. doi:10.1007/s10592-020-01305-2.

Busch, K., Hanz, U., Mienis, F., Mueller, B., Franke, A., Martyn Roberts, E., et al. (2020b). On giant shoulders: How a seamount affects the microbial community composition of seawater and sponges. *Biogeosciences* 17, 3471–3486. doi:10.5194/bg-17-3471-2020.